SAND2016-8618C

Paper # 82

Predicting Polymer Degradation and Mechanical Property Changes for Combined Aging Environments

By Kenneth T. Gillen*
Sandia National Laboratories (retired), P.O. Box 16143
Albuquerque, NM 87191-6143

and Mathew Celina
Sandia National Laboratories, Box 5800
Albuquerque, NM 87185-5800

Presented at the Fall 190th Technical Meeting of
Rubber Division, ACS
Pittsburgh, PA
October 11-13, 2016

ISSN: 1547-1977

*Speaker

ABSTRACT

Accelerated aging models are needed when two environments impact degradation and the current paper considers combined radiation-temperature environments (CRTE). A viable model described in the past is the dose to equivalent damage (DED) model which assumes that in a CRTE, by accelerating the thermal-initiation rate by a factor x (from Arrhenius *T*-only analysis) and raising the radiation dose rate by the same factor x leads to a factor x increase in the combined degradation rate. We critically review and update the DED model, using a 2-D plot that describes the model's underlying framework and how its assumptions can be tested using so-called Matched Accelerated Conditions (MAC) which reflect the simple acceleration factor assumption above. Historical data on several elastomers not only confirms the model assumptions, but shows that substantial degradation chemistry changes occur as one transitions from thermo-oxidative dominated to radiation-dominated degradation. This latter, but not unexpected observation, handled appropriately in the new MAC approach, conflicts with the primary assumption used in an alternative but highly-empirical past model and therefore eliminates this alternate model from consideration.

Given the chemical changes that depend upon the particular mix of radiation plus temperature, accelerated aging simulations should ideally choose accelerated conditions along the MAC line that intersects the ambient conditions, leading to more confident lifetime predictions. Finally we show that these same concepts lead to an approach that allows remaining lifetimes of samples aged under ambient conditions to be derived using a MAC analogy to the Wear-out approach developed previously for thermo-oxidative aging.

INTRODUCTION

Various polymeric materials are expected to last for extended periods of time (often decades) in air environments. For this reason there has been a decades long on-going effort at developing methods for making lifetime predictions using accelerated aging techniques. For materials subjected to air aging at elevated temperatures, we recently published 2 reviews that outlined in great detail some of the problems in making confident lifetime predictions and methods to circumvent these problems.[1,2]

A more difficult and continuing problem is how to make lifetime predictions when two degrading environmental factors are present. In particular we have been interested in this challenge with respect to combined radiation-thermal environments for more than 30 years and derived an approach many years ago that we initially referred to as "Time-temperature-Dose Rate (*t*-*T*-*R*) superposition".[3,4] It is based on the assumption that by accelerating the thermal-initiation rate by a factor x (from Arrhenius *T*-only analysis) and raising the radiation dose rate *R* by the same factor x, this combined acceleration leads to a factor x increase in the combined degradation rate. Because of the way the model was applied to degradation data, the approach is now typically referred to as the Superposition of dose to equivalent damage (DED) data. A second combined $R + T$ model called the "Superposition of time-dependent data" was also suggested many years ago.[5,6] At present, these two approaches are the main methods recommended for making predictions in combined radiation-thermal environments.[7,8]

By examining published and unpublished data from our historic almost 40-year combined environment aging program as well as some new results, we will show that the time-dependent-data approach cannot be applied with confidence to most polymeric materials and that the DED approach can be significantly improved in terms of its capabilities to give confident lifetime predictions. We refer to the improved DED approach as the Matched Accelerated Condition (MAC) approach. It is based on examining the assumptions underlying *t*-*T*-*R* superposition on a plot of experimental conditions in *R*-*T* space (log of *R* versus 1000/*T*) where the MAC concept is introduced. Because of the model assumptions, this plot is effectively identical to the Arrhenius plot of log shift factor or log failure time versus 1000/*T* that is used for thermal-only aging situations. We therefore briefly review the *T*-only approach before attacking the more complex case of $R + T$ environments.

EXPERIMENTAL

MATERIALS

The materials studied were jacketing and insulation materials from commercial cables used in nuclear power plant applications. Table I summarizes the materials examined, giving the Sandia designation, the manufacturer's description, and the ACS Nomenclature (Name and Abbreviation). The reason for including the Sandia designation is because this is the designation used in the Sandia Excel file that contains much of the raw data (published and unpublished) that has been generated on each material. This Excel file of data and a Sandia storage cabinet containing the aged samples are referred to as SCRAPS which stands for "Sandia's Cable Repository for Aged Polymer Samples". The experimental conditions, Lab-book location of raw data plus recordings of the data are included in an Excel file labeled SCRAPSXX.xls which is available from Sandia on request. This file is periodically updated (the

XX denotes the version) and SCRAPS91.xls represents the 91st and most recently available version.

TABLE I
MATERIALS

SCRAPS name	Manufacturer's name and type	ACS name	ACS abbreviation
EPR-01A	Anaconda Flameguard insulation	Ethylene propylene rubber	EPM
Hyp-05	Rockbestos Firewall III jacket	Chlorosulfonated polyethylene	CSM
Hyp-06	Eaton Dekoron Elastoset jacket	Chlorosulfonated polyethylene	CSM
Neo-01	Okonite Okolene jacket	Chloroprene rubber	CR
Neo-02	Rockbestos Firewall III jacket	Chloroprene rubber	CR
Sil-01	Rockbestos Firewall II insulation	Silicone	SI
EPR-03	Eaton Dekoron Elastoset insulation	Ethylene propylene rubber	EPM

DATA SOURCES

For data given in this report that come from published work, references to the source are given. However, many of the dose-dependent results for combined environment aging situations are previously unpublished results obtained from the SCRAPS91.xls file.

RADIATION AGING

Radiation aging was carried out in Sandia's Low Intensity Cobalt Array (LICA) facility. Cobalt-60 pencils contained under water in various stationary arrays irradiate the samples. The samples are held in watertight aging cans that are lowered into the water tank containing the cobalt pencils. This arrangement allows long-term aging exposures (up to 1 year or longer) to be easily conducted. The aging cans are temperature controlled (capabilities are up to 250°C) and monitored through umbilical cables that also allow for gas (air or nitrogen) circulation during the experiments.

TENSILE TESTING

The materials for tensile testing were carefully stripped, before aging, from the low voltage electrical cables. For jacketing samples, the resulting samples were typically ~150 mm long by 6 mm wide by ~1.5 mm thick. After carefully removing the copper conductors the insulation samples were aged as tubes having lengths of ~150 mm. Tensile testing (5.1 cm initial jaw separation, 12.7 cm/min strain rate) was performed on Instron tensile testing machines equipped with pneumatic grips; an extensometer clamped on the sample allowed ultimate tensile elongation values to be obtained. For each aging time in a given environment, three identically aged samples were typically tensile tested with the average value reported and analyzed in the subsequent analyses.

OXYGEN CONSUMPTION

Two techniques have been used and described in detail in earlier publications. One approach uses gas chromatography to determine the amount of oxygen consumed by a sample in a closed container after a given aging exposure.[9] The second approach uses a respirometer.[10]

MODULUS PROFILING

Modulus profiles were obtained on sample cross-sections using a computer-controlled, automated version of our modulus profiling apparatus, which has been described in detail previously.[11,12] The basic procedure typically involves mounting three small pieces of the aged material side by side in a vise-like device. This holder is then metallographically polished yielding smooth polished cross-sections of the three samples. The holder is placed in the apparatus such that a loaded probe with a paraboloidally shaped tip can be used to indent the central sample perpendicular to the cross-sectional surface of this sample. Through the use of a two-step loading procedure, the amount of indentation into the sample can be used (together with the known loading on the probe and the probe tip geometry) to calculate the inverse tensile compliance, a quantity closely related to the tensile modulus of the material. The apparatus allows measurements to be made with a resolution of ~50 μm. By scanning across the sample cross-section, a detailed map of modulus versus probe location is obtained.

GEL CONTENT AND SOLVENT UPTAKE

Solvent uptake measurements were carried out by first exposing a known weight of sample (w_0) to refluxing p-xylene for a minimum of 24 hours. The sample was recovered from the hot solvent and then quickly placed and sealed in a small container of known weight so that solvent evaporating from the sample was trapped in the sealed container. The weight of the swollen rubber (w_s) was then determined from the weight gain of the sealed container. The final weight w_f of the remaining gel was determined after drying the swollen sample under vacuum. The solvent uptake factor is defined as the ratio of w_s to w_f. The percent gel is given by the ratio of w_f to w_0. Typical initial sample weights for these experiments were ~50 mg.

NMR T_2 RELAXATION

NMR T_2 relaxation time measurements were made on the Rockbestos CR material using a Bruker DRX spectrometer at 399.9 MHz as described in previous publications.[13]

RESULTS AND DISCUSSION

BRIEF REVIEW OF THERMAL-ONLY AGING[1]

Historically, a quite common approach to accelerated aging studies in thermos-oxidative (air-containing) environments involved aging the material of interest in several accelerated temperature environments and determining a selected "failure" time at each temperature. If the failure times had the often anticipated Arrhenius behavior, than the times t would have a dependence given by

$$t \propto \exp\left[\frac{-E_a}{RT}\right] \qquad (1)$$

where E_a is the Arrhenius activation energy, R is the gas constant and T is the absolute aging temperature in degrees Kelvin. Plots of the log of the failure times versus inverse absolute temperature would be linear if Arrhenius behavior applied. An example of this approach involves oven-aging studies on an EPDM o-ring. Various degradation properties (tensile elongation, density, modulus, sealing force) were found to change slowly until very large

changes occurred simultaneously at the so-called induction time. When the log of the induction times for all four variables were plotted versus inverse absolute aging temperature, linear behavior resulted as seen in Figure 1.[1,14] The typical approach would then be to extrapolate the linear (Arrhenius) behavior to ambient conditions, predicting a lifetime of ~55,000 years at 25°C.

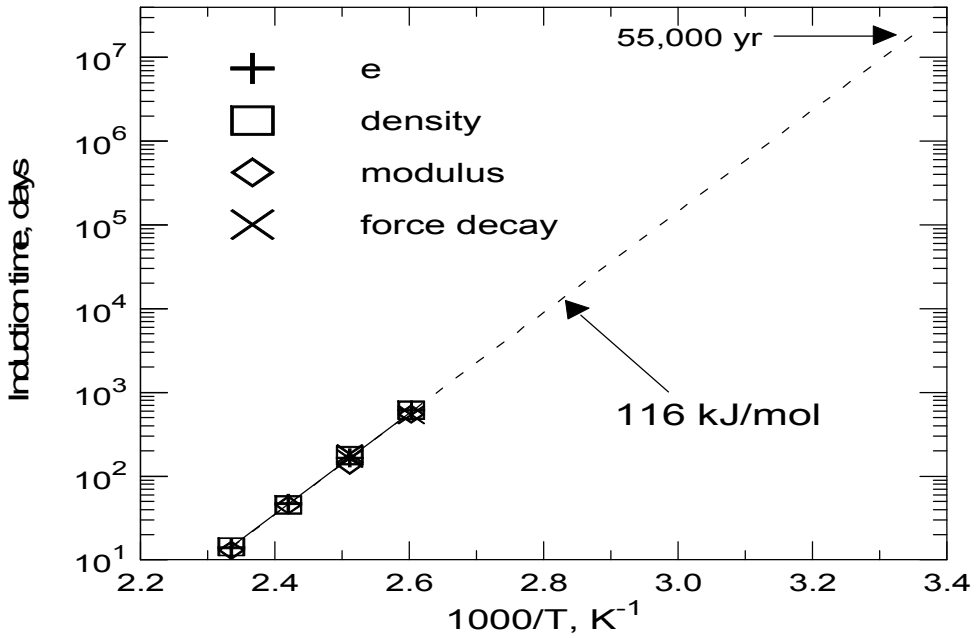

Figure 1. Arrhenius plot of induction times for an EPDM o-ring material.

Although excellent linear (Arrhenius) behavior is obvious, this rather simplified approach raises three important issues.

1) Is there evidence that the degradation chemistry is changing as the accelerating temperatures change?
2) Since diffusion-limited oxidation (DLO) is typically absent under ambient conditions and becomes more important as the aging temperature is raised,[15,16,17] does DLO have an effect on the analysis?
3) How do we get more confidence in such long extrapolations?

In our recent review[1], we showed how each of these issues can be addressed in a reasonable fashion, resulting in more confidence in extrapolated predictions of thermal-oxidative situations. To find evidence that the degradation chemistry is only accelerated but mechanistically unchanged as the accelerating temperature is increased, we recommended carrying out time-temperature superposition analyses[18] where the results from the various accelerating temperatures are multiplicatively shifted to one temperature to see if reasonable superposition occurs. Reasonable superposition over the accelerating temperature range offers evidence for unchanging degradation chemistry. As an example, we show time-temperature superposed results for the Okonite CR jacket for oven-aging experiments ranging from 70°C to 161°C (and limited 24°C results) in Figure 2. The incredible superposition over such an extended temperature range gives compelling evidence for unchanged degradation chemistry at least from 161°C through 70°C.

When the superposition shift factors a_T are plotted on an Arrhenius plot (log of a_T versus inverse absolute temperature), the results (Figure 3) indicate nice Arrhenius behavior (E_a ~ 89 kJ/mol) from 161°C down to 70°C with a small drop in E_a at lower temperatures, a drop consistent with results for numerous materials.[1]

For this material, we often[1] only show data up to 121°C because important DLO effects enter at higher temperatures (especially at 131°C and higher as indicated by the vertical dashed line in Figure *3*. But in the present discussion, we include the higher temperature results in the important DLO region to address the second issue concerning DLO effects. The importance of DLO at 131°C and above can be seen from modulus profiling results. Modulus profiling results at 131°C are shown in Figure 4 where *P* gives the percentage of the cross-section from the outside sample surface to the inside sample surface.[19] Oxidation proceeds at normal equilibrium with the oxygen in air at the surfaces (no DLO effects) but DLO leads to lower oxidation and slower increases in modulus in interior regions. During tensile testing, cracks will initiate at the hardened outside surface (P = 0%) and immediately propagate through the cross-section so the elongation results are unaffected by DLO. The tensile strength, on the other hand, measures the force at break integrated across the entire cross-section so it would be expected to be affected by DLO. This is the case as seen from tensile strength results (Figure 5) shifted using the same shift factors appropriate to elongation, where non-superposition clearly enters at higher temperatures. This shows that one must be careful attempting to model data when DLO effects are present by either eliminating DLO effects (use small enough material cross-sections if possible) or choosing a degradation parameter that is unaffected by DLO (e.g., elongation when oxidation hardens the material more than DLO reductions in oxidation harden the material).

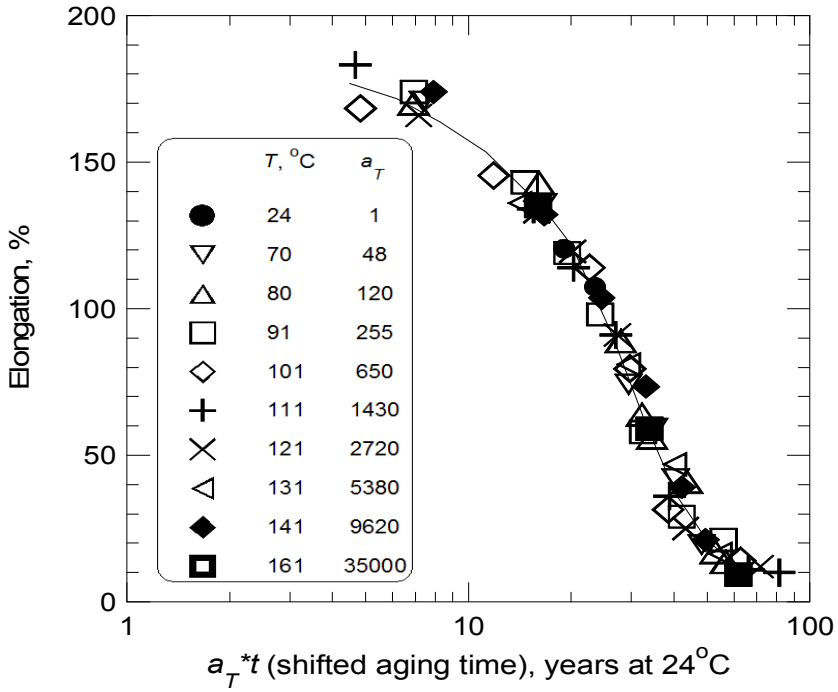

Figure 2. Time-temperature superposition of Okonite CR results.

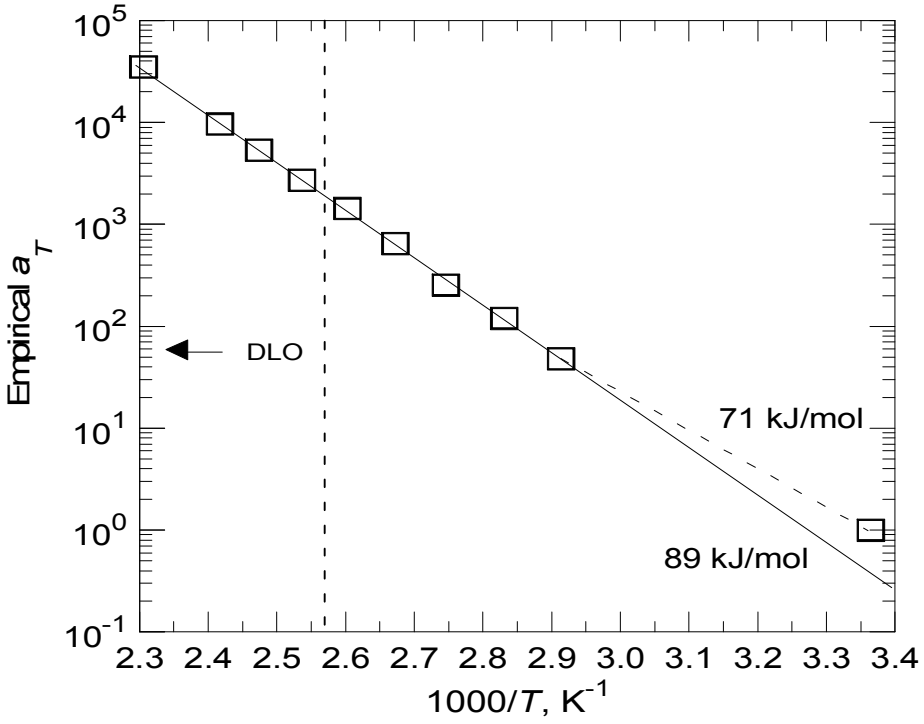

Figure 3. Arrhenius plot of experimental shift factors for Okonite CR material.

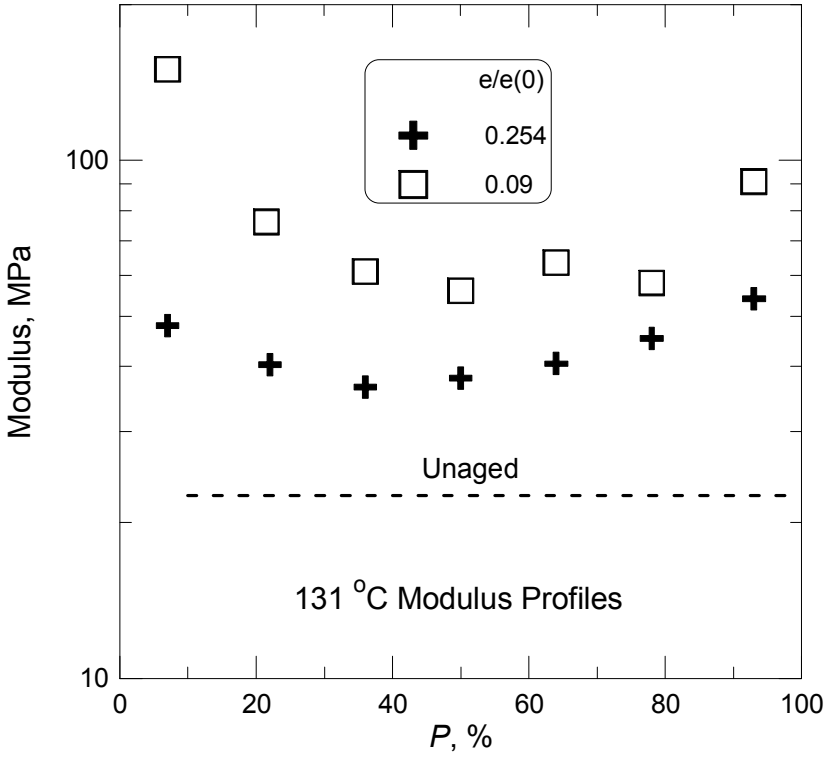

Figure 4. Modulus profiles across cross-section for Okonite CR material at 131°C.

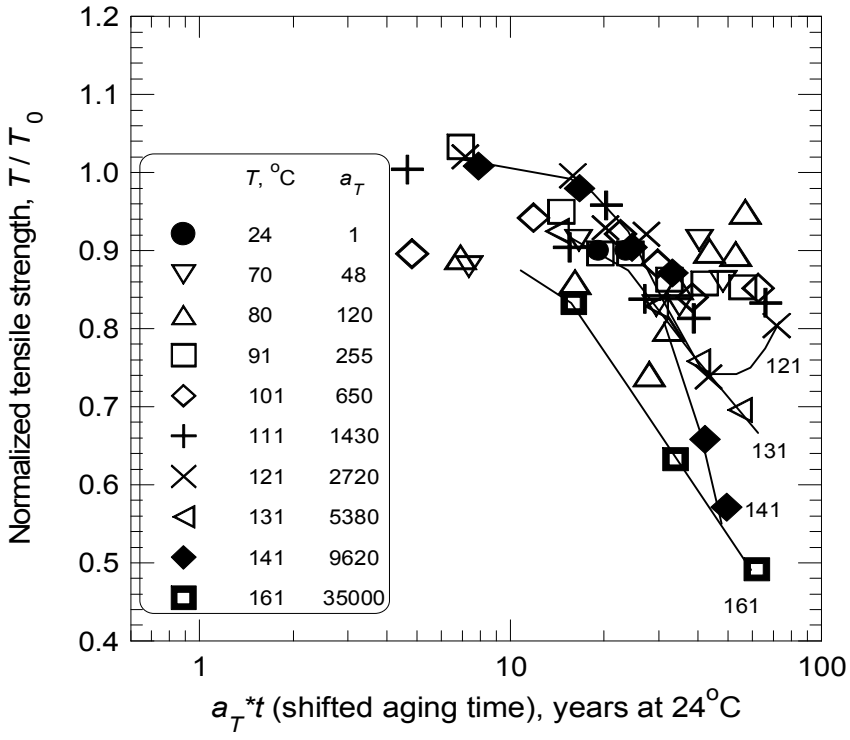

Figure 5. Normalized Tensile strength data for Okonite CR material shifted using the a_T values appropriate to the elongation.

Finally, we showed in our recent review[1] that oxygen consumption measurements can be made from the normal accelerated temperature regime down to temperatures approaching ambient and that such measurements offer a method of gaining confidence in the long extrapolations usually involved when attempting to use high temperature results to make predictions at ambient, use temperatures. We will see below how we handle the same three issues in the more complex case of combined radiation plus temperature aging.

AIR-AGING IN RADIATION PLUS TEMPERATURE ENVIRONMENTS

When radiation (e.g., high energy gamma) is added to temperature for air-aging of polymers, the situation becomes much more complex. The initiation step for thermal-only aging is the formation of free radicals at a thermally weak region of the polymer chain. With gamma radiation, the higher energy involved leads to a more diverse set of free radical species.[20] Thus one would expect that the degradation chemistry would vary as one moves in *R*-*T* space from a radiation-dominated regime (high dose-rate, low temperature) to a temperature dominated regime (low or non-existent radiation, high temperature). As usual, such differences should be discernable from differing shapes of degradation versus time or dose curves when plotted versus log time or log dose. We examine this expectation below for four different elastomers by comparing results taken where *R* dominates (high dose rates and low temperatures) with results taken where *T* dominates (lower dose rates and higher temperatures).

Figure 6 shows results for the Anaconda EPM insulation comparing similar dose rates applied at high and low temperatures where temperature is much more important for the former conditions and radiation is more important for the latter conditions. Clearly the shape differences show that

the chemistry changes, dependent upon which environment is more important, consistent with our expectations.

Figure 7 shows results for the Okonite CR material comparing the most radiation-dominated conditions with the most temperature-dominated conditions. Again the significant differences in shape are consistent with our expectations of differing chemistry in the two limits. For both of these first two materials, the degradation rate is faster in the *T*-dominated regime.

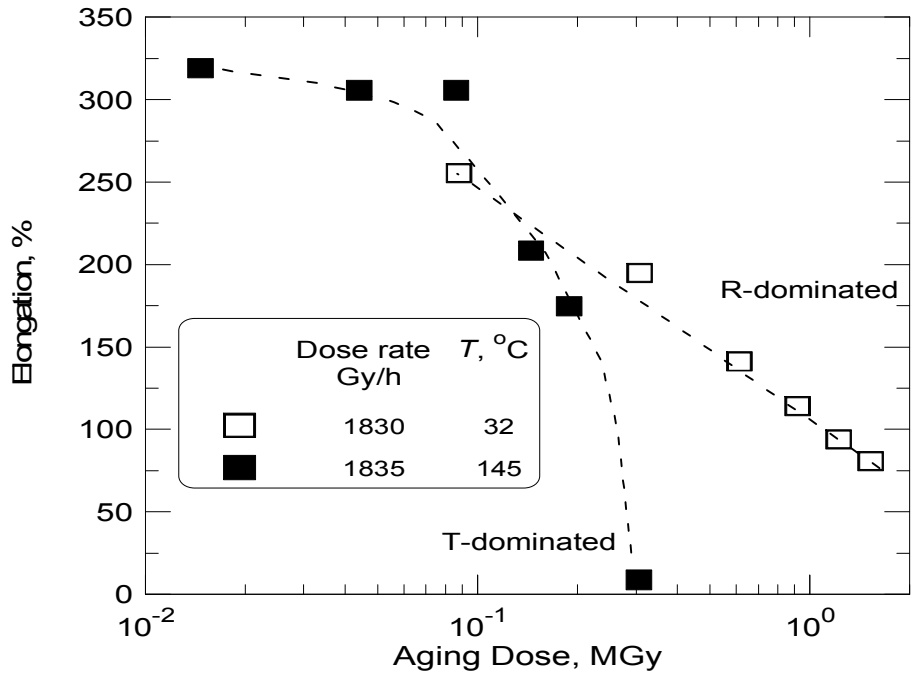

Figure 6. Elongation vs radiation dose for the Anaconda EPM under *R*-dominated and *T*-dominated aging conditions.

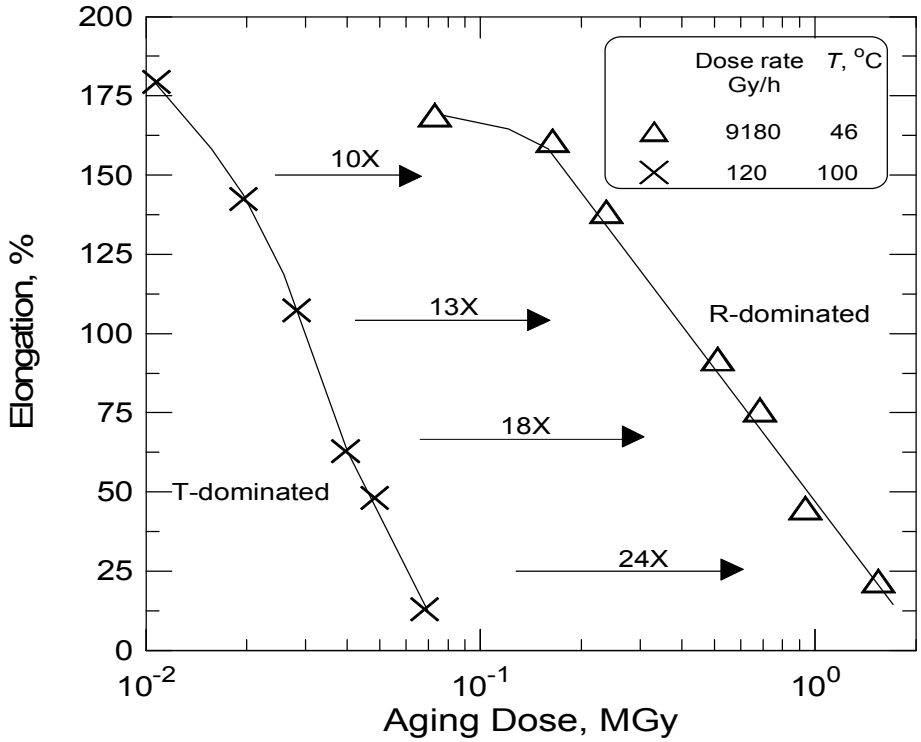

Figure 7. Elongation vs radiation dose for the Okonite CR under *R*-dominated and *T*-dominated aging conditions.

Similar conclusions about the expected differences in chemistry as one goes from *R*-domination to *T*-domination are obvious for the Rockbestos CSM and the Rockbestos SI as seen from data in Figure 8 and Figure 9. For these two materials, the chemical degradation rate is faster in the *R*-dominated regime, the opposite of the situation for the EPM and CR materials.

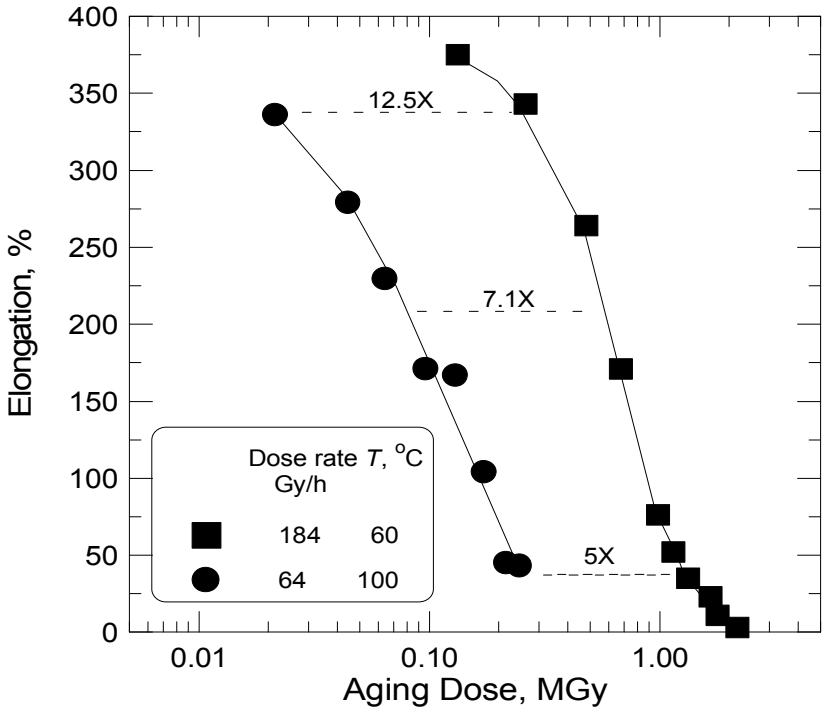

Figure 8. Elongation vs radiation dose for the Rockbestos CSM under *R*-dominated and *T*-dominated aging conditions.

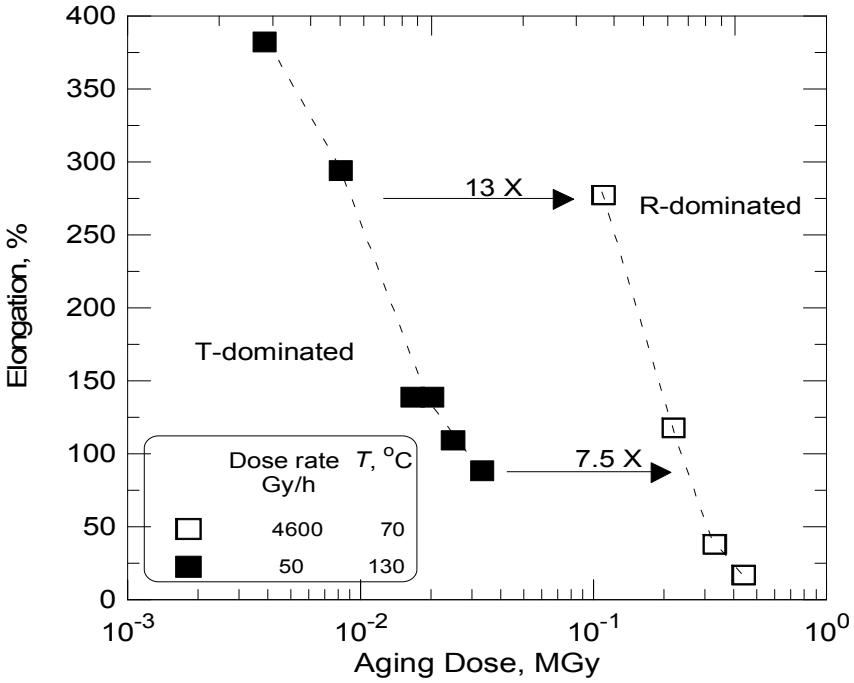

Figure 9. Elongation vs radiation dose for the SI under *R*-dominated and *T*-dominated aging conditions.

HISTORICAL MODELING OF RADIATION + THERMAL ENVIRONMENTS

As mentioned above, there are two main models that have been applied to analyzing combined radiation plus thermal environments. The so-called time-dependent model[5,6,7,8] proposes the following combined environment shift factor for combined temperature (T) and Radiation dose rate (R)

$$\alpha(T,R)=\frac{\exp(-E)}{R_g}\left(\frac{1}{T}-\frac{1}{T_{ref}}\right)\left(1+\frac{kR^x\exp Ex}{R_g}\left(\frac{1}{T}-\frac{1}{T_{ref}}\right)\right) \quad (2)$$

where E is the activation energy for thermal only degradation; k and x are empirical constants and R_g is the gas constant. This totally empirical model assumes the same chemistry occurs throughout R-T space and IEC and IAEA documents note this limitation by explicitly stating[7,8]

"This empirical model can only be used for those materials where the shape of the damage parameter versus log time curve does not change with temperature and dose rate…. If the curve shape changes, superposition of data is not possible and the method cannot be used."

The results shown in the previous section offer compelling evidence that this assumption is usually wrong. As noted earlier, the failure of this assumption should be anticipated given the differences in initiation steps expected for T-initiation versus R- initiation.

The other model often applied was originally referred to as time-temperature-dose rate superposition[3,4] but later became known as the "Superposition of DED data" based on the way it was applied to data analysis. It is based on a simple assumption that says if one increases the temperature initiation rate by a factor x (from the Arrhenius acceleration factor for thermal only experiments) and at the same time one increases the radiation initiation rate by the same factor x (by increasing the dose rate R by the factor x), the resulting combined environment initiation rate and therefore the overall chemistry degradation rate will be increased by the same factor x.[3,4] It is important to note that the dose rate assumption (increasing the dose rate by a factor x increases the radiation degradation chemistry by a factor x) implies that dose rate effects (DRE) are unimportant. The important implications of this observation will be discussed below.

Over the past several decades, we have taken combined environment air-aging data on numerous cable jacketing and insulation materials. Since we recognized that the chemistry (shape) changed as one went through R-T space, we applied the so-called DED approach using the same simplistic assumption (1 failure point per curve) used on Figure 1 for T-only cases. Thus we typically looked at a value of the elongation (usually either 50% or 100%) that constituted "failure". This resulted, for instance, in us determining the dose required to reach a certain "failure" elongation which would be referred to as the dose to equivalent damage (DED). The analysis starts with plots of the DED data points (y-axis) versus the log of the dose rate (x-axis) with the aging temperature noted and marked for each data point. An example for the Anaconda EPM material is shown on Figure 10 where the DED refers to the dose required to reduce elongation to 100%.

In order to use the model to predict "failure" by extrapolation to lower environmental conditions, we note that the thermal-only E_a for this material was measured as 106 kJ/mol.[21] The procedure

involves horizontal shifting of the data points from their temperature and dose-rate conditions to the temperature and dose rate of interest assuming the model assumptions hold. For instance, to shift the result at 145°C + 1835 Gy/h from Figure 10 to 50°C, we use the 106 kJ/mol E_a to determine that the appropriate shift factor for temperature is a factor of 7802. The model therefore says that the dose rate should be dropped by this same factor from 1835 Gy/h to 0.235 Gy/h so the 145°C + 1835 Gy/h data is shifted to 50°C as shown in Figure 11.

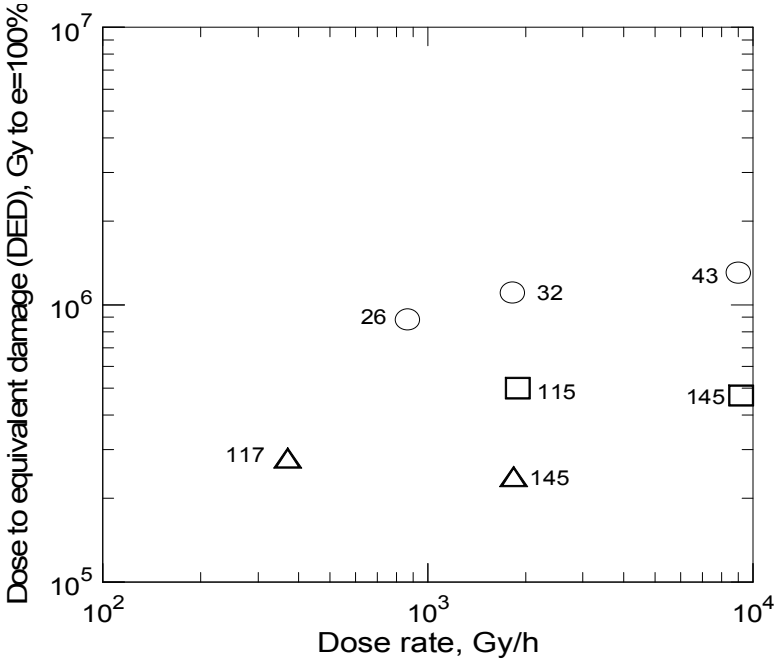

Figure 10. Radiation dose to reach 100% elongation versus dose rate for the Anaconda EPM (numbers indicate aging temperature in °C).

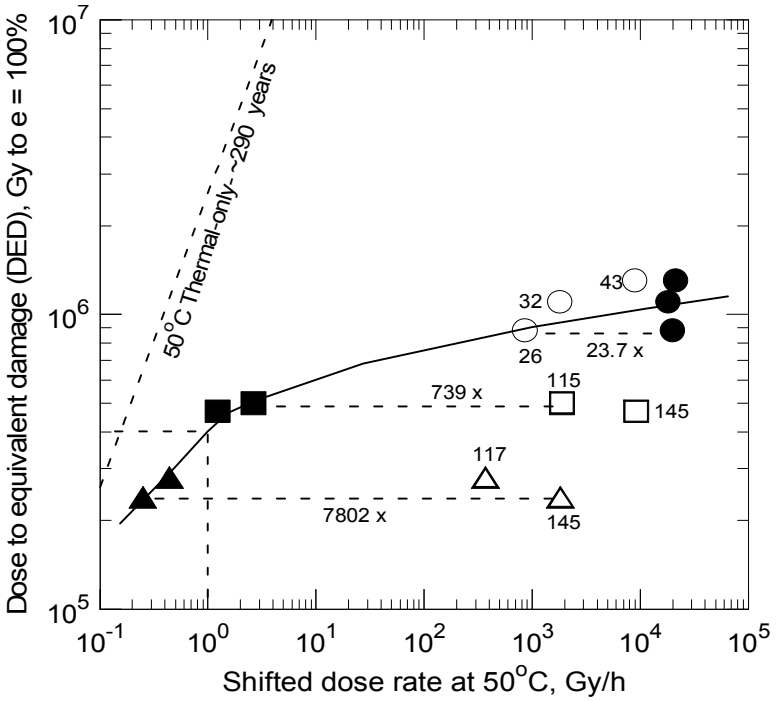

Figure 11. Shifting procedure for the Anaconda EPM DED results to make predictions at 50°C.

Similar procedures are used to shift all of the remaining data points, resulting in the filled symbols, the curve through which represents the predicted curve for "failure" at 50°C and dose rates ranging from 0.25 Gy/h to 2e4 Gy/h. Towards the low dose region, the results are approaching the thermal-only 50°C predicted line and at higher dose rates the results reflect moving towards domination by radiation.

Although one can be somewhat confident in the predicted extrapolated results when the shifted results fall close to the same curve, in effect the same issues that were raised for the simplified thermal-only approach (Figure 1) hold for Figure 11. We already know that the degradation chemistry changes as we move from *R*-domination towards *T*-domination so what effect does this have on the extrapolations? Again DLO can be a concern. Finally, we would like to have a better approach to gain more confidence in the very large extrapolations. Our new improved MAC approach attacks these issues.

IMPROVED COMBINED ENVIRONMENT APPROACH

Introduction to the Matched Acceleration Conditions (MAC) approach.- The improved approach involves using the time-temperature-dose rate (*t*-*T*-*R*) superposition model assumptions to create a plot of the experimental *R*-*T* conditions with log of dose rate *R* plotted versus the inverse absolute temperature as shown in Figure 12.

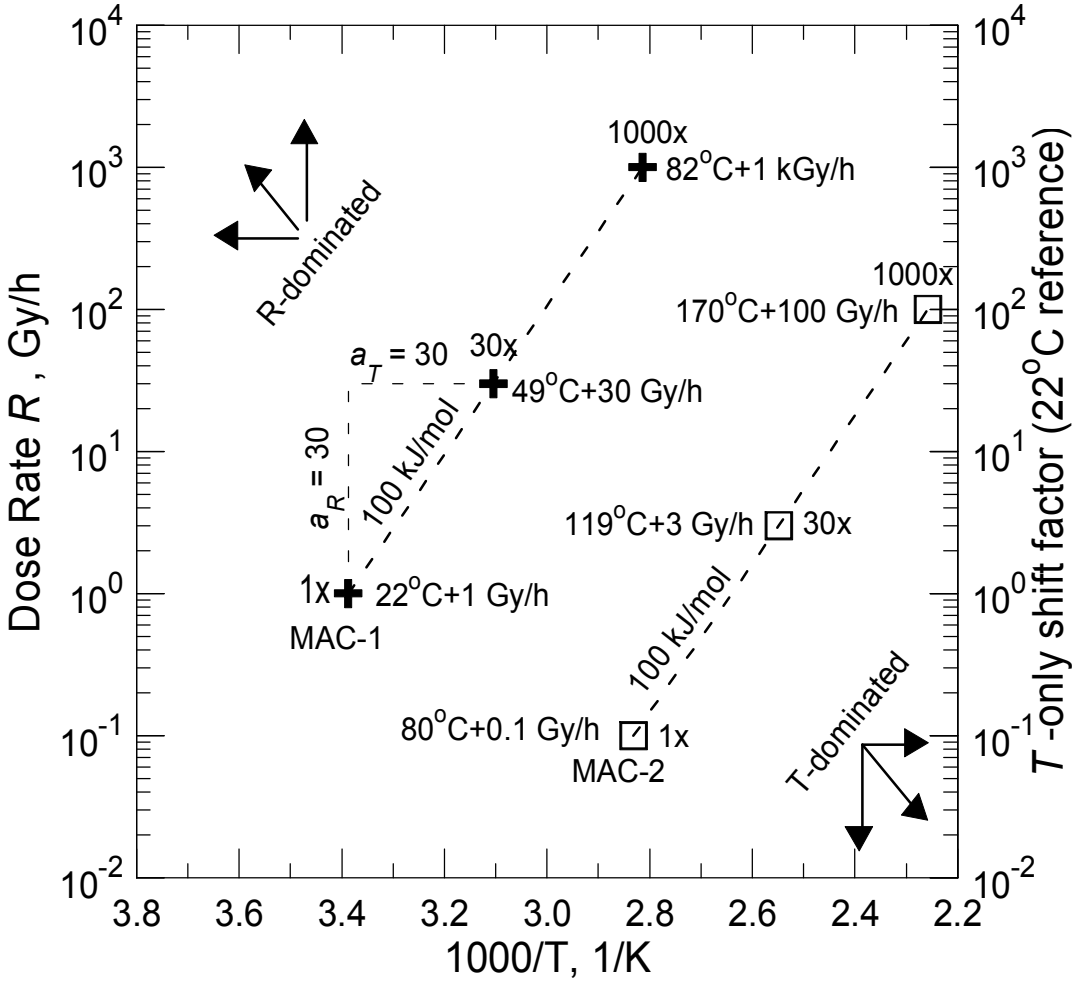

Figure 12. Plot of log Dose Rate versus 1000/T for E_a of 100 kJ/mol showing Matched Accelerated Condition (MAC) lines.

At high dose rates and low temperatures, the radiation environment will dominate the degradation as indicated by the arrows at the upper left of the plot. Similarly at low dose rates and high temperatures, the thermal environment will dominate the degradation a indicated by the arrows at the lower right of the plot. Suppose the *T*-only E_a is 100 kJ/mol and we are concerned about simulating *R*-*T* aging at 22°C + 1 Gy/h. Using this E_a we can calculate *R*-*T* conditions for various accelerations. Note that the *t*-*T*-*R* model is based on equal accelerations of temperature and radiation initiation so the Arrhenius acceleration factor from 22°C + 1 Gy/h to higher combined *R*-*T* conditions is identical to the acceleration factor for radiation as indicated by the right-hand y-axis. Points along this line are referred to as Matched Accelerated Conditions (MAC). In a similar way we can find the MAC line appropriate to accelerations from an *R*-*T* aging condition of 80°C + 0.1 Gy/h. These lines are labeled MAC-1 and MAC-2, respectively with the former closer to *R*-domination and the latter closer to *T*-domination. The assumptions of the model assume that the chemistry appropriate to a given MAC line is unchanged. Thus data taken at 22°C + 1 Gy/h should degrade 30 times slower than data taken at 49°C + 30 Gy/h. Therefore if these two sets of data are plotted versus radiation dose, the model assumptions say they should superpose. Similarly data taken along the MAC-2 line should also superpose. Since MAC-1 is closer to *R*-domination and MAC-2 is closer to *T*-domination and we know that shape changes from MAC-1 to MAC-2 would therefore be expected, this approach can potentially handle such shape changes. The key is determining whether superposition (identical chemistry) occurs along a MAC line.

Anaconda EPM Results.- Combined environment aging conditions for Anaconda EPM are shown on Figure 13 together with 3 MAC lines drawn through the data locations using its E_a of 106 kJ/mol.

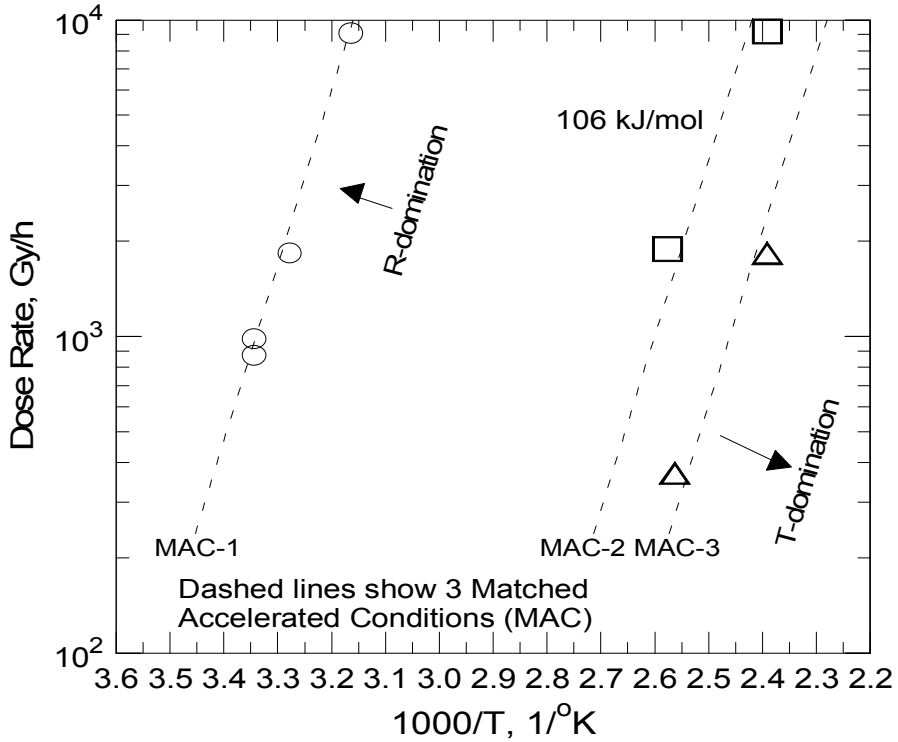

Figure 13. Dose rate + temperature aging conditions for the Anaconda EPM material.

The 2 triangles and the 4 circles lie reasonably close to the MAC-3 and MAC-1 lines, respectively and represent the experiments closest to *T*-domination and *R*-domination. When the tensile elongation results for the experiments denoted by circles (approaching *R*-domination) and those denoted by triangles (approaching *T*-domination) are plotted versus radiation dose (Figure 14), we see excellent superposition occurs along the MAC lines with very distinct shape differences between those along MAC-1 versus those along MAC-3. This is compelling evidence for the assumptions underlying the MAC approach.

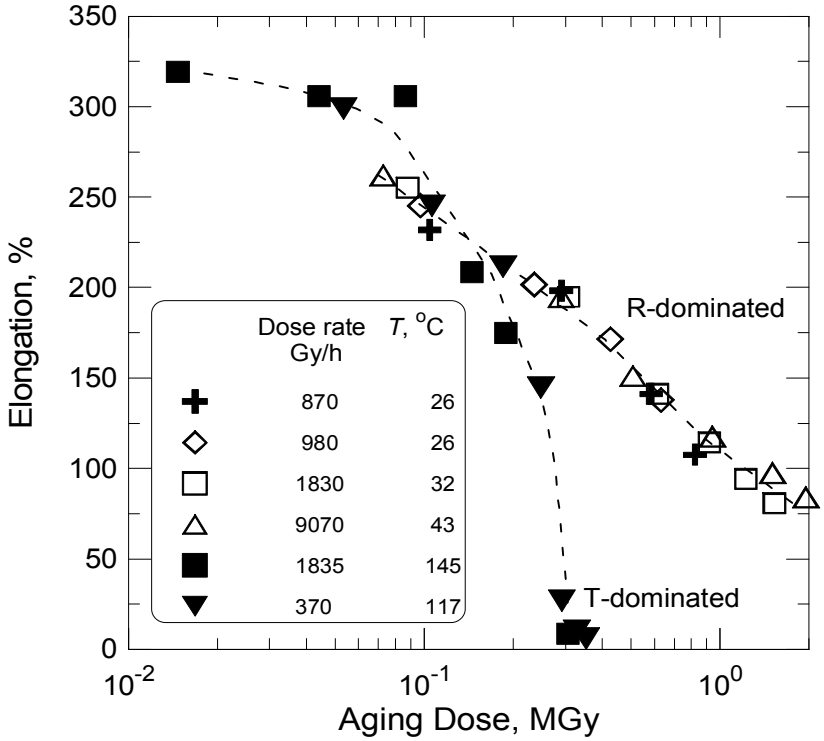

Figure 14. Anaconda EPM elongation versus radiation dose results along the MAC-1 line (*R*-dominated) and the MAC-3 line (*T*-dominated).

Okonite CR Results.- The next material of interest to MAC analysis is the Okonite CR material described earlier since this material was studied extensively in 23 combined radiation plus temperature environments and many of these environments were influenced by important DLO effects.[3] These data will therefore allow us to see whether the new approach gives reasonable superposition for degradation versus dose along MAC lines and how DLO effects impact such data. We start by using our latest estimates[22] of combined environment oxygen consumption and oxygen permeability for typical commercial CR materials in order to estimate the aging conditions influenced by DLO effects. The oxygen consumption (∅) and oxygen permeability (P_{Ox}) estimates[23] are shown in Figure 15 and Figure 16. We can use these estimates together with the following equation from DLO theory[24] to determine which of the 23 experiments are likely to be influenced by DLO effects. The equation gives the limiting sample thickness L_c if one wants to guarantee that the integrated oxidation across the sample cross-section is at least 90% of the homogeneously oxidized case. With a typical β value of ~3, L_c is given by

$$L_c = 2\sqrt{\left(\frac{pP_{Ox}}{\emptyset}\right)} \qquad (3)$$

where p is the oxygen partial pressure surrounding the sample on both sides during the aging (13.2 cmHg in high-altitude Albuquerque). This allows us to estimate the experiments influenced by DLO effects. Figure 17 shows the MAC-oriented plot of the dose-rate and temperature conditions for the 23 experiments together with a solid curve delineating the division between the heterogeneous region where DLO effects are expected to enter and the homogeneous region unaffected by DLO.

Evidence in support of the curve separating the DLO region from the non-DLO region comes from published oxidative penetration measurements made with polishing techniques.[25] These experimental measurements were made on the room temperature aged CR samples at 470 Gy/h + 24°C and 84 Gy/h + 22°C. Comparisons of the experimental results for the total oxidation distance L_{Ox} from both edges (twice the measured oxidative penetration distance) versus the calculated L_c values from eq. (3) are given in Table II. Given the excellent agreement between experimental and theoretical values, it appears that the theory does a good job of predicting where DLO is important. Given that the typical thickness of this CR material is ~1.5 mm, it is clear that the experiment at 22°C + 84 Gy/h is barely in the DLO region as indicated in the figure.

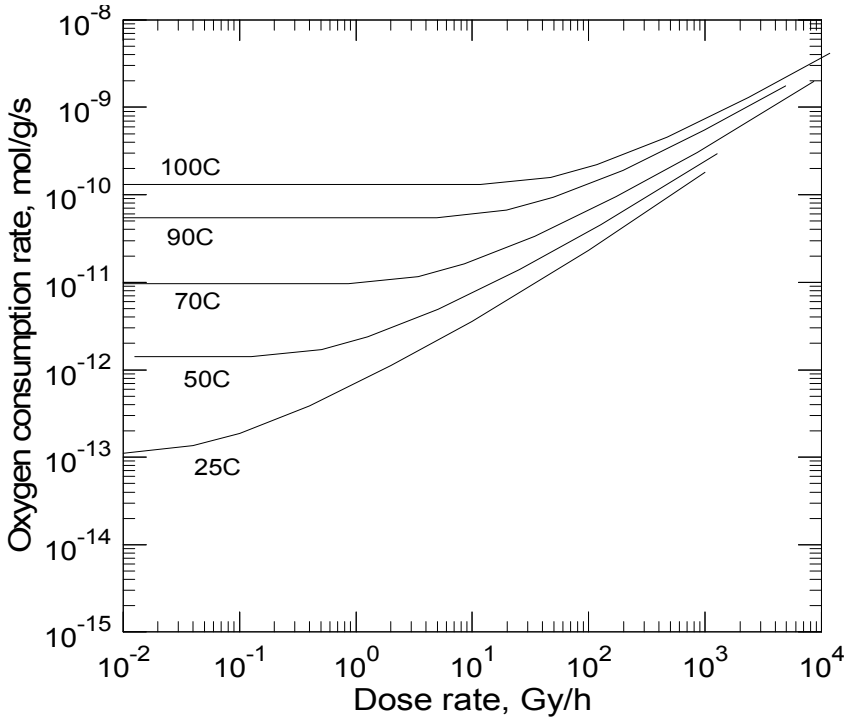

Figure 15. Estimates of oxygen consumption (Ø) versus combined environment aging conditions for the Okonite CR cable jacketing material.

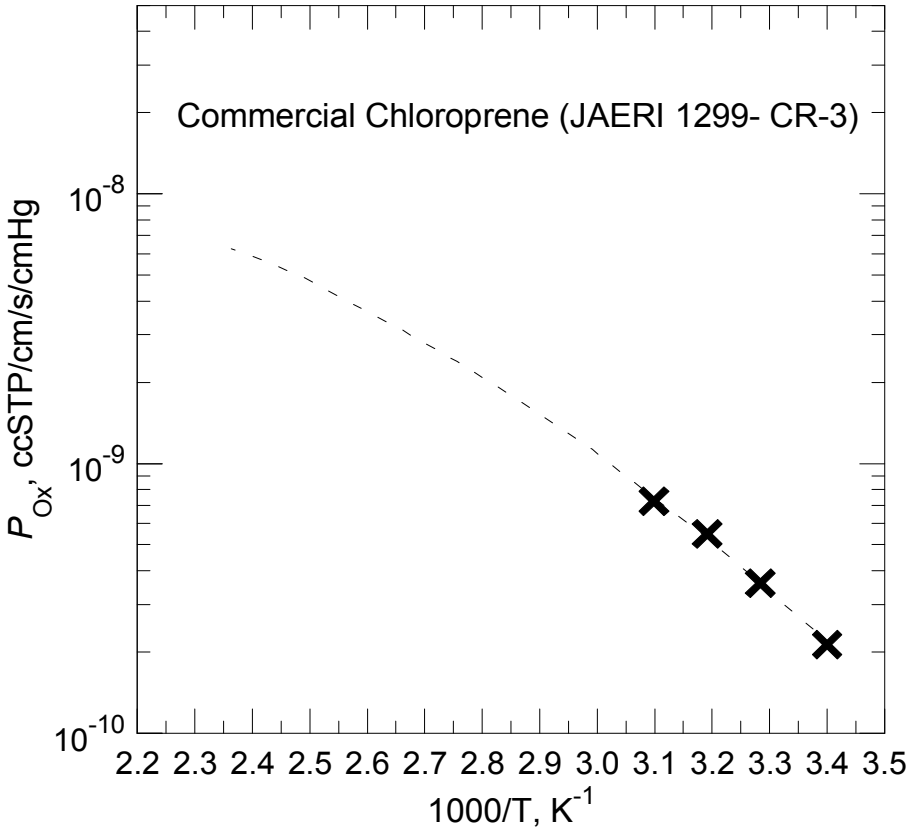

Figure 16. Temperature-dependent oxygen permeability P_{Ox} for a commercial CR cable material.

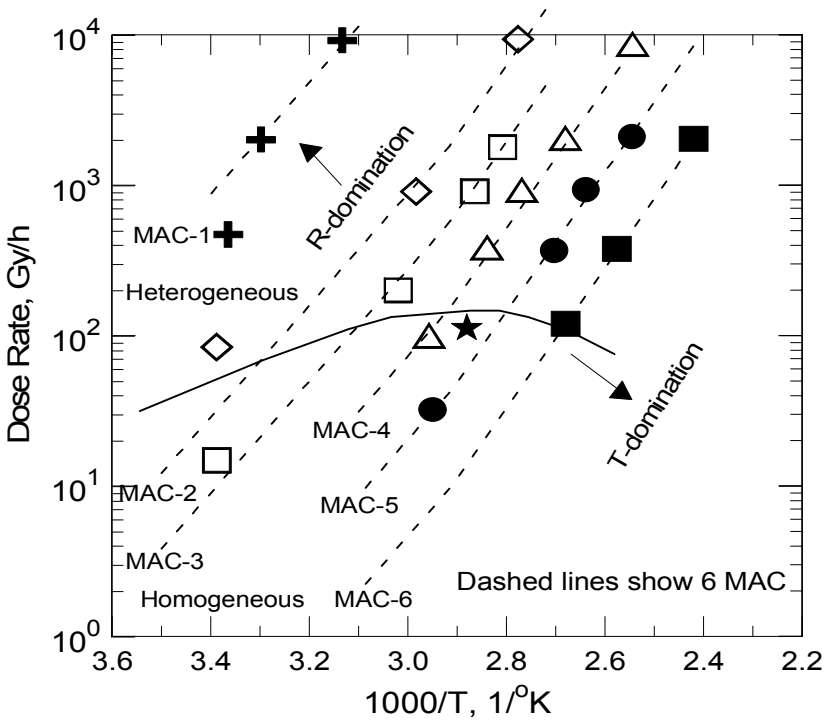

Figure 17. Dose rate + temperature aging conditions for the Okonite CR material with the solid curve separating the estimated region where DLO effects are likely (marked heterogeneous).

TABLE II.

Experimental versus theoretical oxidation distance into CR from both surfaces.

Temperature, °C	24	22
Dose rate, Gy/h	470	84
L_c , mm (theory)	0.69	1.40
L_{Ox} , mm (experimental)	0.68	1.44

Six MAC lines are drawn on Figure 17 using the experimental slopes from the Arrhenius plot of Figure 3 with an attempt to make each line approximately encompass several data conditions. The data conditions appropriate to each MAC line are denoted by the same symbols so, for instance, the MAC-1 line uses crosses, the MAC-2 line uses diamonds, etc. Figure 17 indicates that most of the experiments on each of the 6 MAC lines are influenced by DLO effects. Therefore, we need to choose a degradation parameter that is unaffected by DLO effects. We have seen that elongation measurements achieves this goal for many materials that harden faster under oxidation conditions so that the oxidative hardening at the surface (uninfluenced by DLO) determines elongation. With this in mind, Figure 18 shows CR elongation results versus radiation dose for the 3 experiments near MAC-1 (closest to *R*-domination) and the 3 experiments near MAC-6 (closest to *T*-domination).

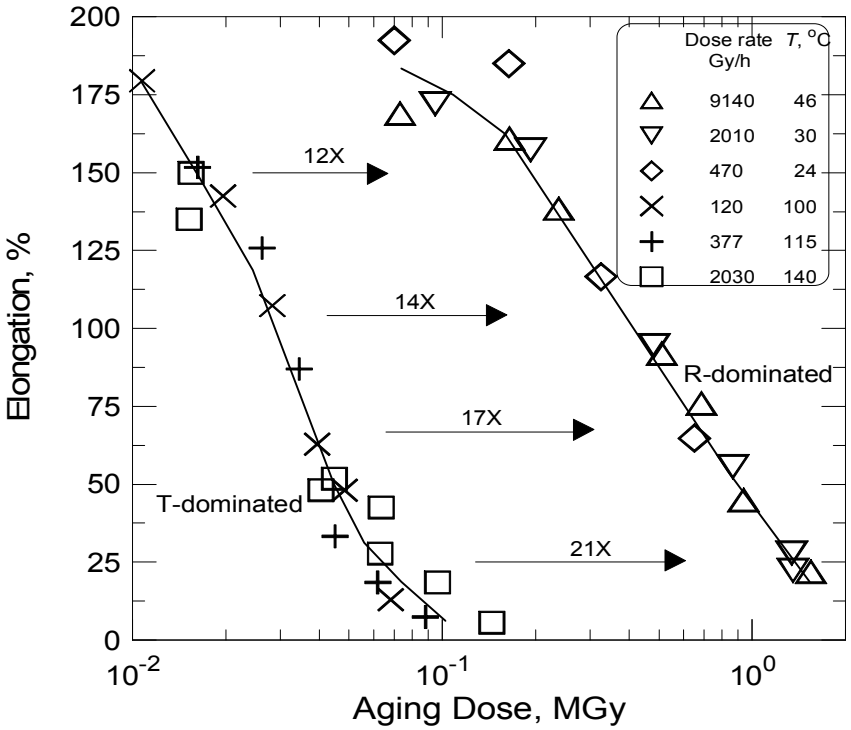

Figure 18. CR elongation versus radiation dose results along the MAC-1 line (*R*-dominated) and the MAC-6 line (*T*-dominated).

The excellent superposition observed under approximate MAC-1 and MAC-6 conditions again gives strong evidence in favor of the assumptions underlying the *t*-*T*-*R* superposition approach. Figure 17 shows that DLO is important for almost all 6 of the experimental conditions plotted in Figure 18 but the use of elongation, a DLO-insensitive parameter when oxidative hardening

dominates, eliminates this problem. Given the prevalence of DLO for most of these experimental conditions, it is interesting to see the effects of using a DLO-sensitive parameter. In particular we next look at normalized tensile strength which will be affected by DLO by examining both elongation and tensile strength for the aging conditions along each of the 6 MAC lines. The results are shown in the next 6 figures, preceding from results close to *R*-domination (MAC-1) to results close to *T*-domination (MAC-6).

As expected, the results for non-DLO influenced elongation measurements for all 6 MAC lines offer compelling evidence for the new approach. The results for tensile strength shows the complicating effects that can occur due to DLO effects when a degradation parameter sensitive to DLO effects is used as a degradation parameter.

Figure 25 summarizes the six superposed elongation curves versus radiation dose drawn through the results for MAC-1 through MAC-6. As one moves in *R*-*T* space from an area near *R*-domination (MAC-1) towards an area near *T*-domination (MAC-6), the dose required for degradation drops substantially. This is not surprising since *T*-initiation reactions will become more important to the overall degradation relative to *R*-initiation reactions as this transition occurs. Perhaps more important is the observation that *T*-initiation reactions will always be present when samples are exposed to radiation environments. We will see the implications of this observation in the next section.

Implications of MAC analysis on experiments looking for Dose Rate Effects (DRE).- For many years researchers have been probing radiation experiments looking for evidence of Dose Rate Effects (DRE). Early on, the simple assumption was that degradation in radiation might depend solely on the total dose received independent of dose rate, often stated as "equal dose, equal damage". This seemed like a reasonable assumption since increasing the dose rate would seem to simply increase the initiation rate in a linear fashion. There was a concern that the free radicals initiated on different tracks might interact more strongly as the dose rate increased, leading to DRE. In fact, evidence for DRE has been reported in numerous publications[5,6,7,8] including some early work by Sandia.[26] It turns out that many of these studies are likely in error by not recognizing the potential importance of *T*-initiation contributions taking place during the experiments. This is because most of these studies involved approximately constant low temperature (e.g., room temperature) exposures versus dose rate. The problem with such experiments is that temperature effects become more important relative to radiation effects as the dose rate is lowered. As an example, we can go back to the Okonite CR combined environment experiments (Figure 17) and look at elongation versus dose results for the three lowest temperature experiments (22°C + 15 Gy/h, 22°C + 84 Gy/h and 24°C + 470 Gy/h). Although the results, plotted in Figure 26, indicate DRE, the apparent DRE are due to movement towards more contribution from *T*-initiation as the dose rate is lowered, resulting in reductions in doses required for a given level of degradation.

MAC analyses takes care of this problem since experiments along a MAC line accelerate both initiation channels equally with the assumption that *R*-initiation is linear with dose rate (e.g., the absence of DRE). Given the excellent superposition along all 6 of the CR MAC lines, it is clear that true DRE do not exist either at low aging temperatures or at high aging temperatures, confirming the originally expected "equal dose, equal damage" hypothesis. A similar conclusion

can be made for the Anaconda EPM material since superposition along MAC-1 and MAC-3 lines was found. Therefore, if one wants to probe for true DRE, the MAC approach must be utilized.

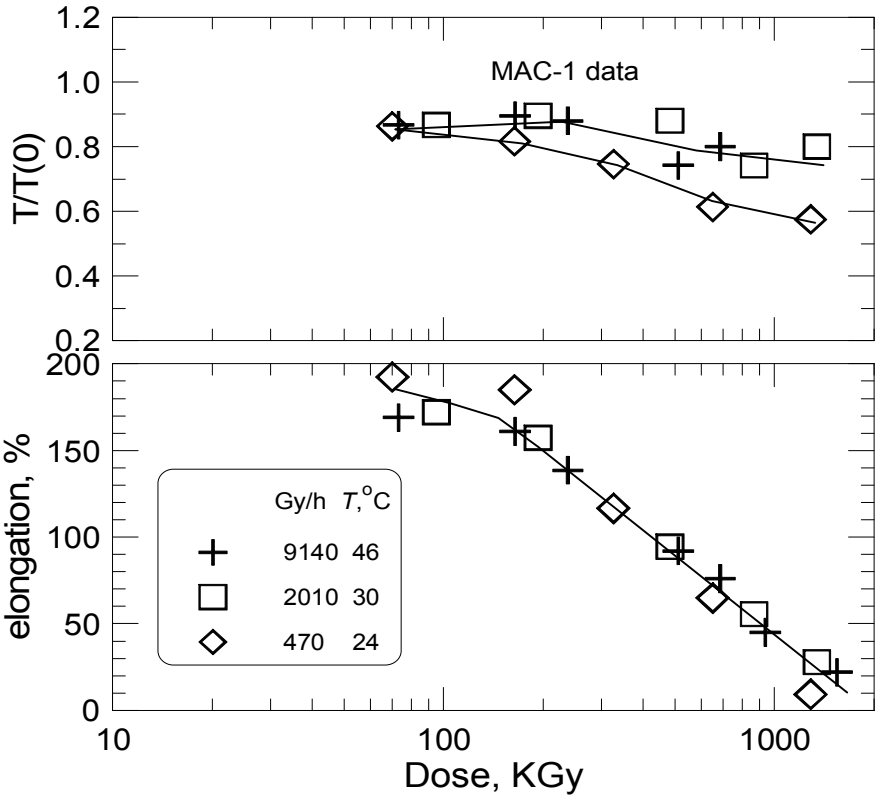

Figure 19. Elongation and normalized tensile strength results for the CR material under experimental conditions close to the MAC-1 line on Figure 17.

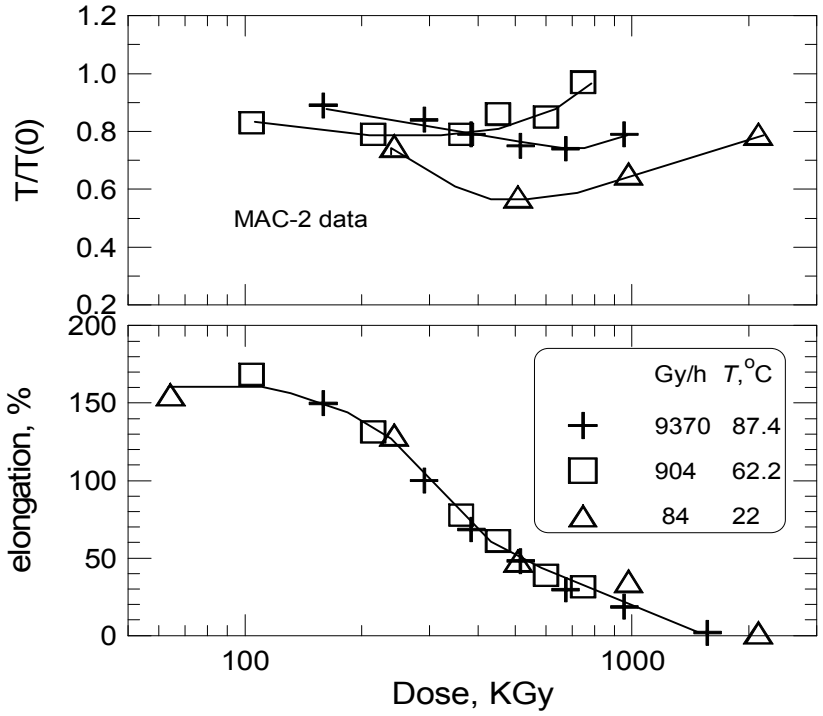

Figure 20. Elongation and normalized tensile strength results for the CR material under experimental conditions close to the MAC-2 line on Figure 17.

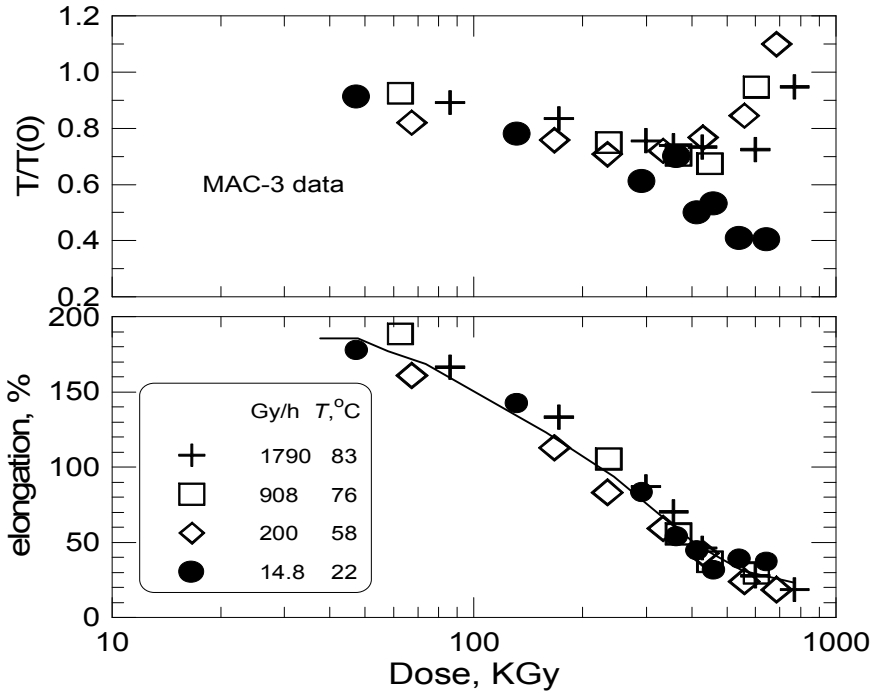

Figure 21. Elongation and normalized tensile strength results for the CR material under experimental conditions close to the MAC-3 line on Figure 17.

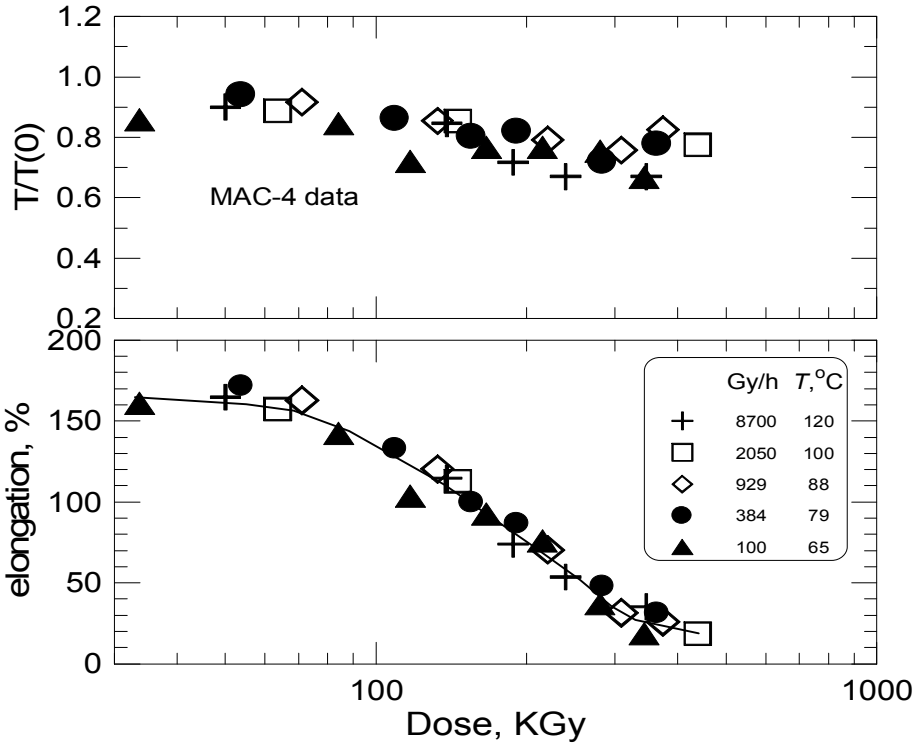

Figure 22. Elongation and normalized tensile strength results for the CR material under experimental conditions close to the MAC-4 line on Figure 17.

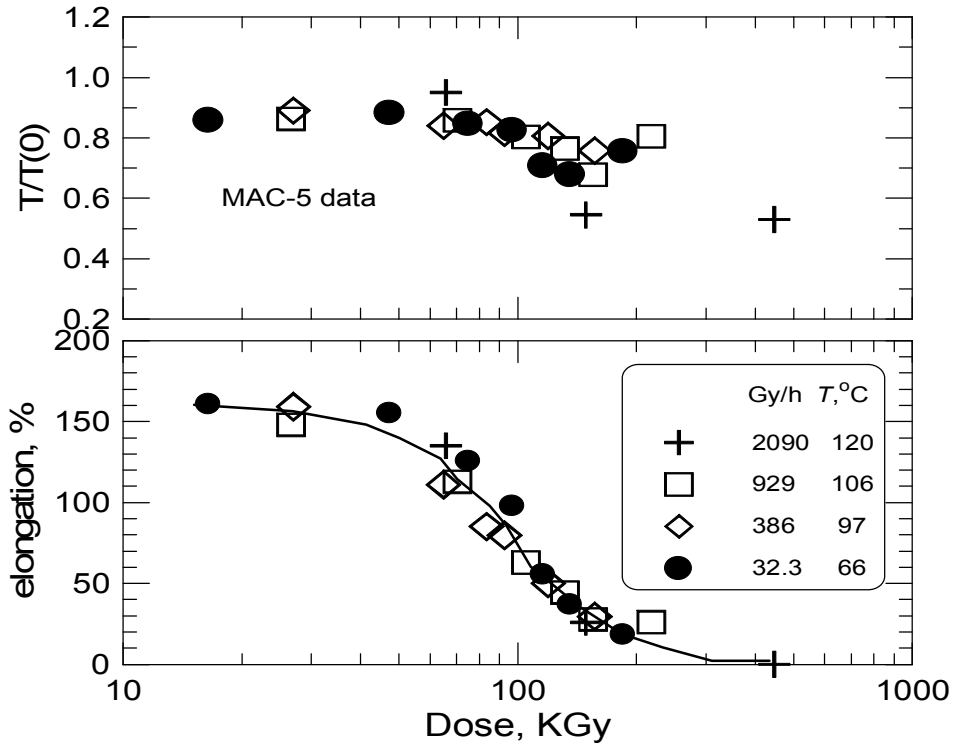

Figure 23. Elongation and normalized tensile strength results for the CR material under experimental conditions close to the MAC-5 line on Figure 17.

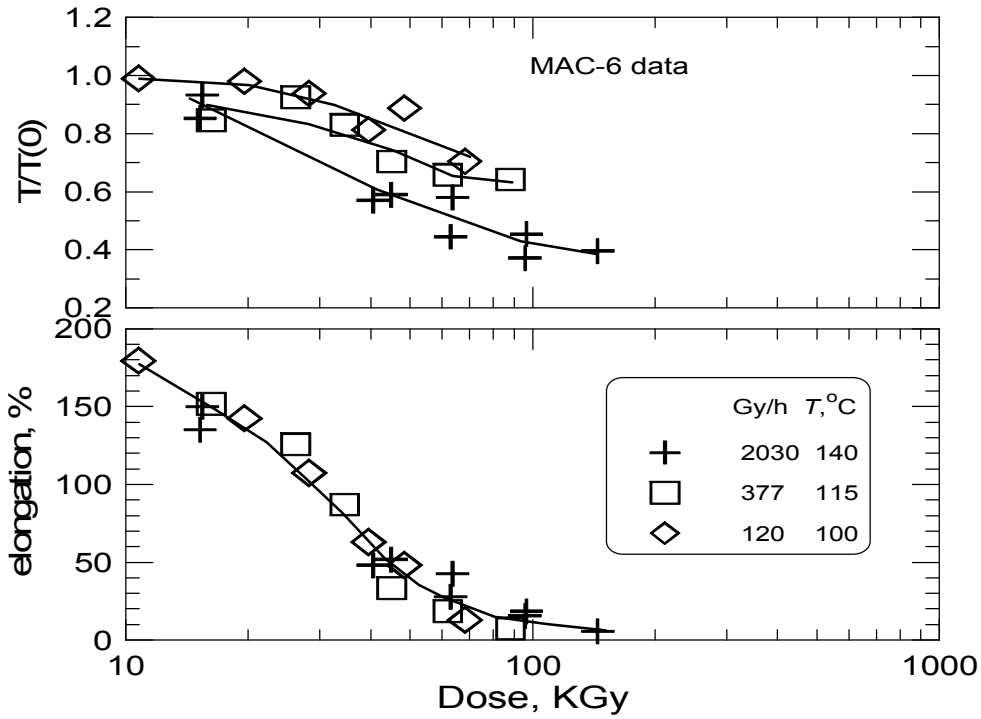

Figure 24. Elongation and normalized tensile strength results for the CR material under experimental conditions close to the MAC-6 line on Figure 17.

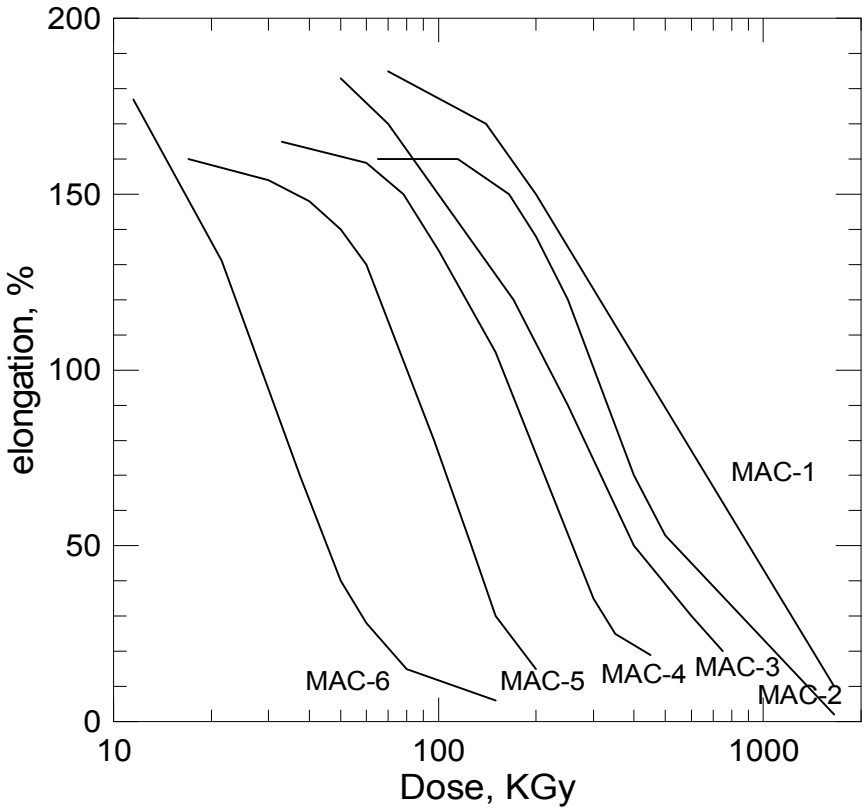

Figure 25. Summary of CR superposed elongation curves for MAC-1 through MAC-6.

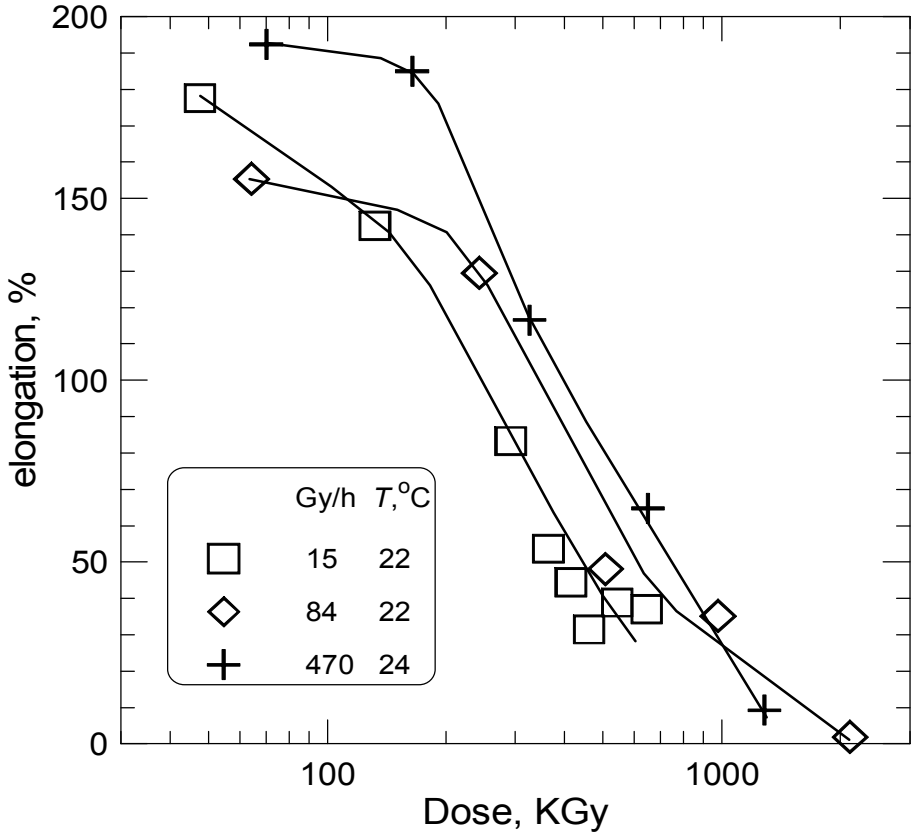

Figure 26. Okonite CR elongation results at the indicated conditions.

Eaton CSM Results.- Over the years, Sandia has studied 9 different CSM cable jacketing and insulation materials. When normalized to 100°C, Arrhenius shift factor plots of oven air-aging results for all 9 materials show excellent agreement with E_a values of ~107 kJ/mol above 100°C and 91 kJ/mol below this temperature as seen in Figure 27.[22] Some limited combined *R*+*T* experiments were run on the Eaton CSM and they are plotted on a MAC plot of interest to the new model in Figure 28. Using the E_a of 91 kJ/mol appropriate under 100°C, three MAC lines are drawn; only MAC-1 has two data locations reasonably close to a MAC line. Figure 29 looks at the shape of elongation results for the 2 data sets along MAC-1 (close to *R*- domination), the superposed *T*-only results (*T*-domination) and the single data set on MAC-2 (intermediate between *R*- and *T*-domination). In this case, there is a small but definite difference in degradation shape, again implying chemistry changes as one traverses *R*-*T* space. It is also clear that the two data sets that are close to the MAC-1 line again give evidence for the *t*-*T*-*R* model assumptions.

Given the excellent agreement with the new model of the elongation results for the two data sets close to MAC-1, the supposition that the degradation chemistry remains unchanged along a MAC line implies that other, non-DLO influenced degradation parameters should show similar superposition when plotted versus dose. Since surface properties are unaffected by DLO, the surface modulus (which determines when elongation failure occurs) should superpose for these two data sets and it does as seen in Figure 30.[27]

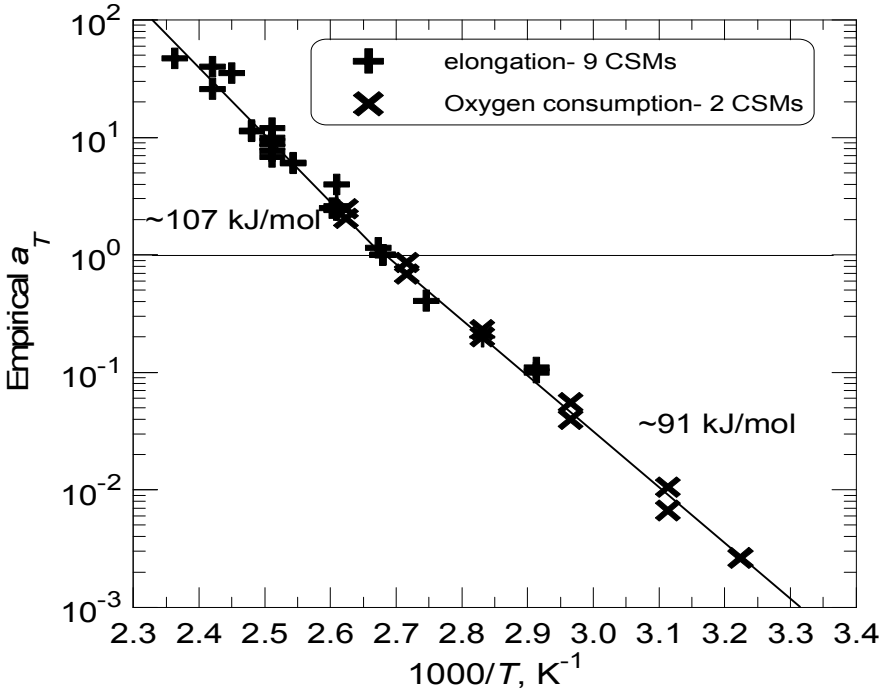

Figure 27. Arrhenius plot of the empirically derived shift factors for elongation for nine CSM materials and the shift factors for oxygen consumption for two CSMs (all data normalized to 100°C).

Gel and uptake factor measurements average across the entire cross-section so any important DLO effects should affect these results. Based on modulus profiles,[27] the experiment at 145 Gy/h + 60°C is unaffected by DLO and the experiment at 1000 Gy/h + 90°C has only slight DLO effects very late in the degradation (for doses above ~ 0.9 MGy where the elongation is below ~50%). With this in mind, results versus dose for these two experimental conditions are plotted

in Figure 31 and Figure 32. As expected, excellent agreement with the MAC approach is observed except for some minor differences for the gel data in the later stages of degradation where DLO begins to enter.

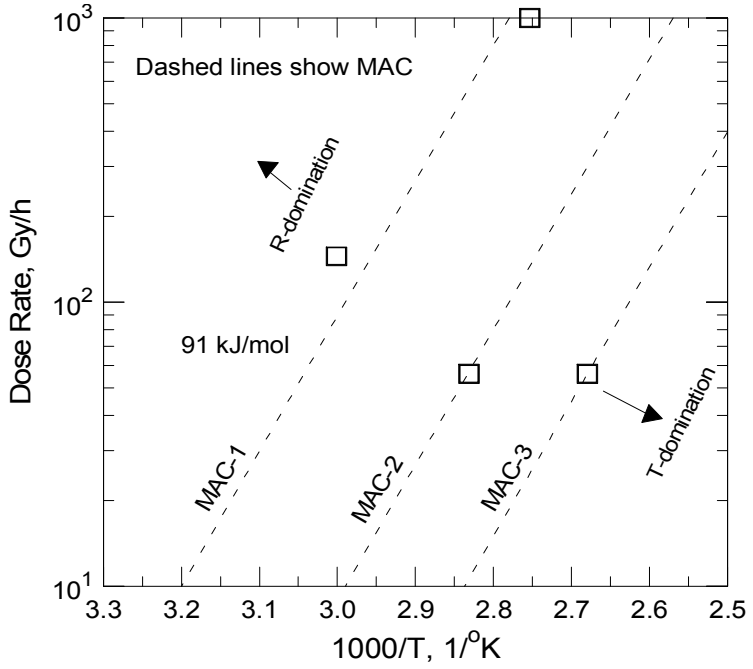

Figure 28. Dose rate and temperature aging conditions for the Eaton CSM material.

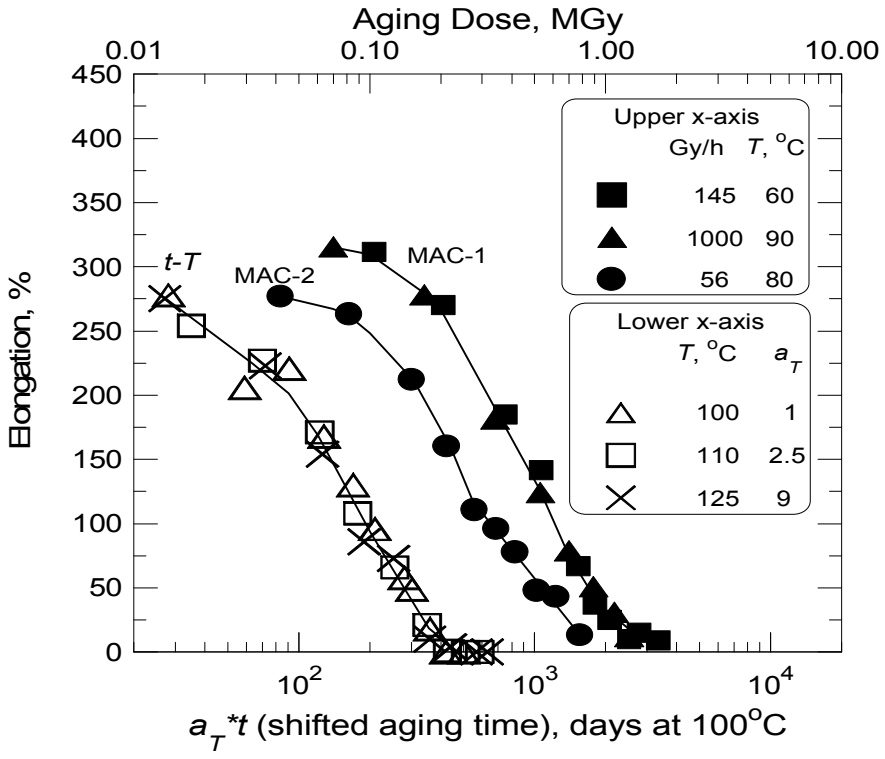

Figure 29. Elongation data for Eaton CSM- *t-T* superposed thermal aging (bottom x-axis) and data from along MAC-1 and MAC-2 (upper x-axis).

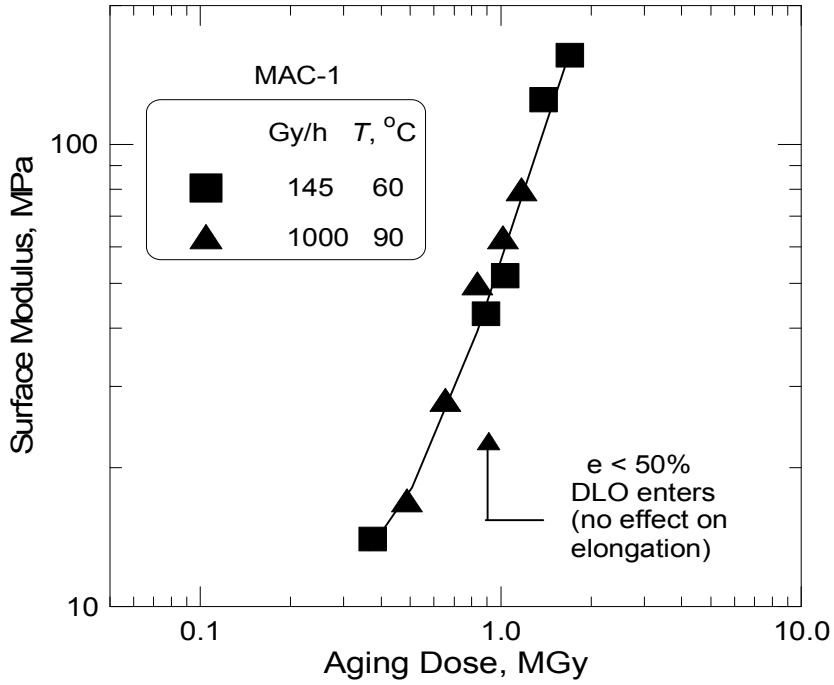

Figure 30. Surface modulus results from modulus profiling versus dose for the two Eaton CSM experiments close to the MAC-1 line.

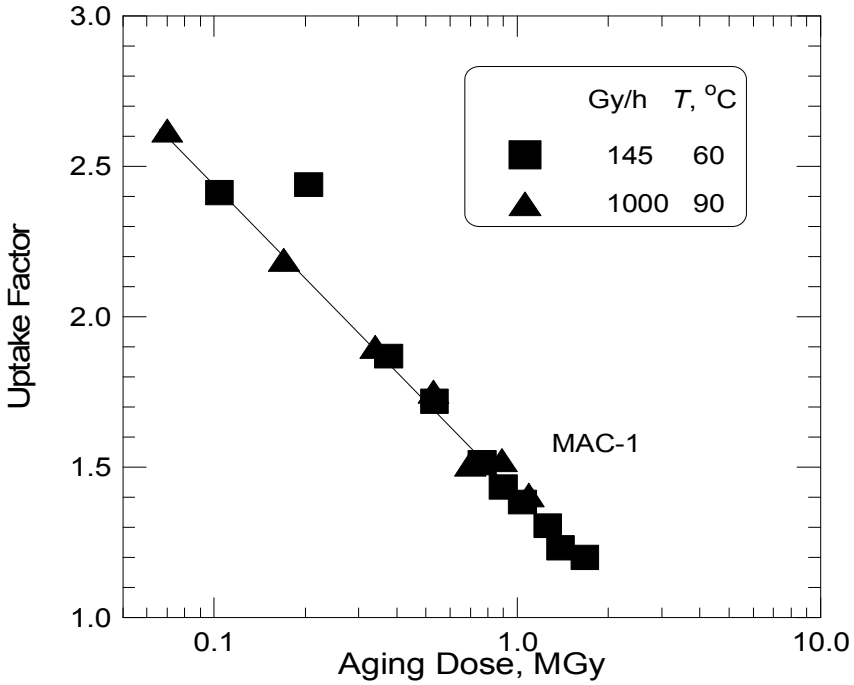

Figure 31. Uptake factor results versus dose for the two Eaton CSM experiments close to the MAC-1 line.

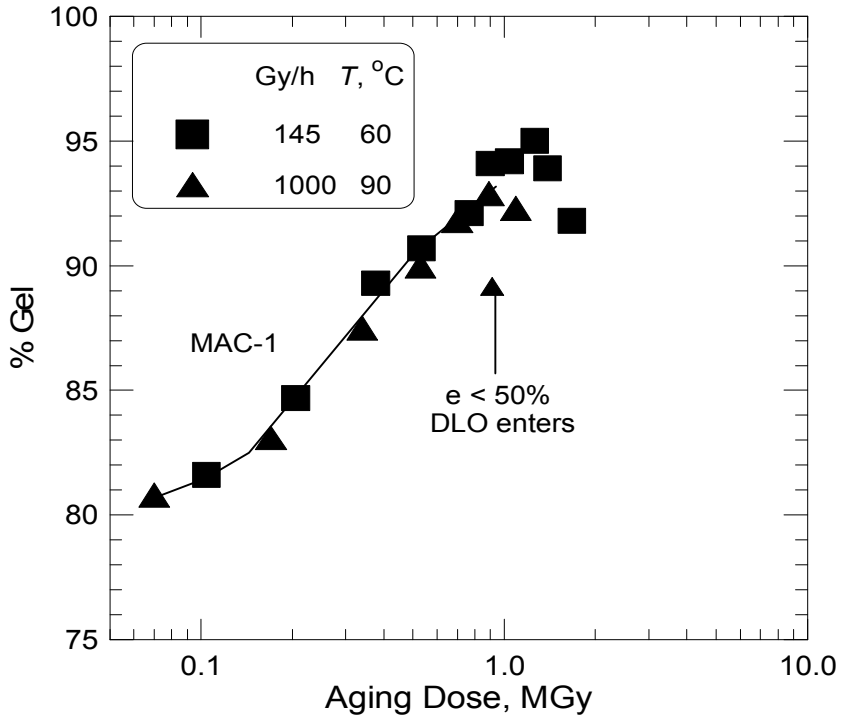

Figure 32. Gel results versus dose for the two Eaton CSM experiments close to the MAC-1 line.

Rockbestos CR Results.- The results for the Rockbestos CR jacketing material are particularly interesting since, as shown below, elongation measurements across *R*-*T* space appear to have similar degradation shapes, so at first glance, one might be tempted to apply the empirical time-dependent model to make extrapolated predictions. Figure 33 shows the Arrhenius *T*-only plot of elongation and oxygen consumption results,[28] where it is seen that an E_a of 86 kJ/mol applies to the temperature range from 80°C down to 37°C. Figure 34 shows the four *R*+*T* experimental conditions plotted on a MAC style plot with a MAC line of slope 86 kJ/mol drawn through two of the experimental conditions. Elongation versus dose results for those two experimental conditions (938 Gy/h + 70°C and 138 Gy/h + 50°C) plus the experiment closest to *T*-domination (43 Gy/h + 80°C) are plotted in Figure 35 (upper x-axis) together with the time-temperature superposed *T*-only results (lower x-axis with same span as upper x-axis).

It is clear from this plot that the shapes of the degradation curves for this material are similar across *R*-*T* space, implying that the empirical time-dependent model might be applicable. However, by examining the correlation of other degradation parameters with elongation, it can be seen that the chemistry does in fact change in *R*-*T* space. In particular we look at uptake and NMR T_2 results both of which could be affected by DLO effects but we note that such DLO effects turn out to be unimportant for the four *R*+*T* aging conditions in Figure 34.[27] The results are shown in Figure 36 and Figure 37. It is clear from these results that there is no evidence suggesting that the chemistry underlying the two experiments on the MAC-1 curve changes since both uptake and NMR T_2 correlate similarly with elongation for the two aging conditions, a conclusion consistent with all of the earlier results shown in this paper. On the other hand, the change in correlation under the *R*+*T* condition closer to *T*-domination shows that the chemistry is changing across *R*-*T* space. Therefore, even though one might be tempted to use the empirical

time-dependent approach based on elongation shape similarities, this would not be advised for prediction purposes.

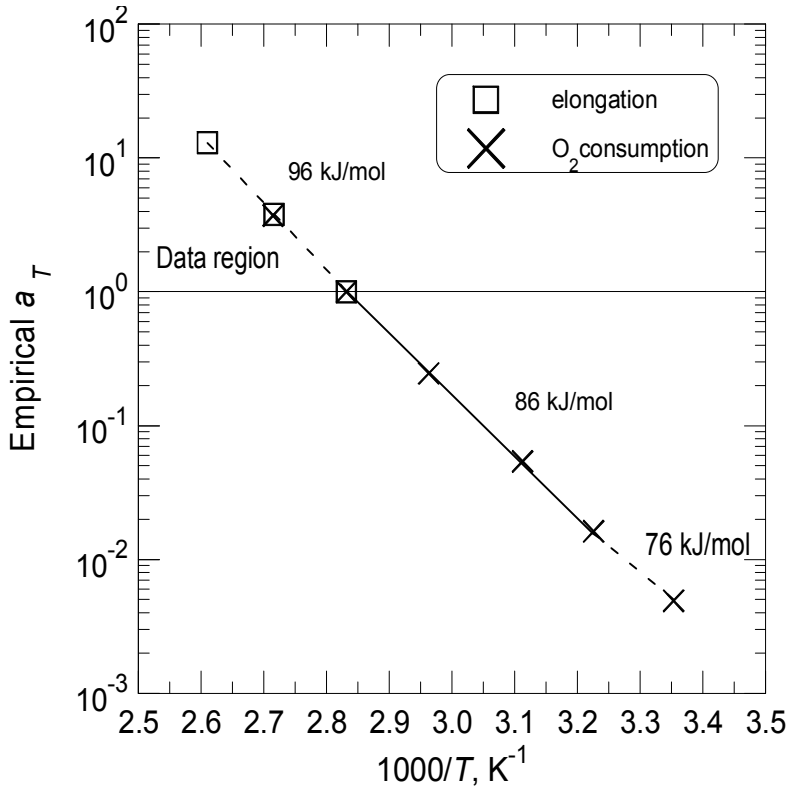

Figure 33. Arrhenius plot of the elongation and oxygen consumption shift factors for air oven aging of Rockbestos CR.

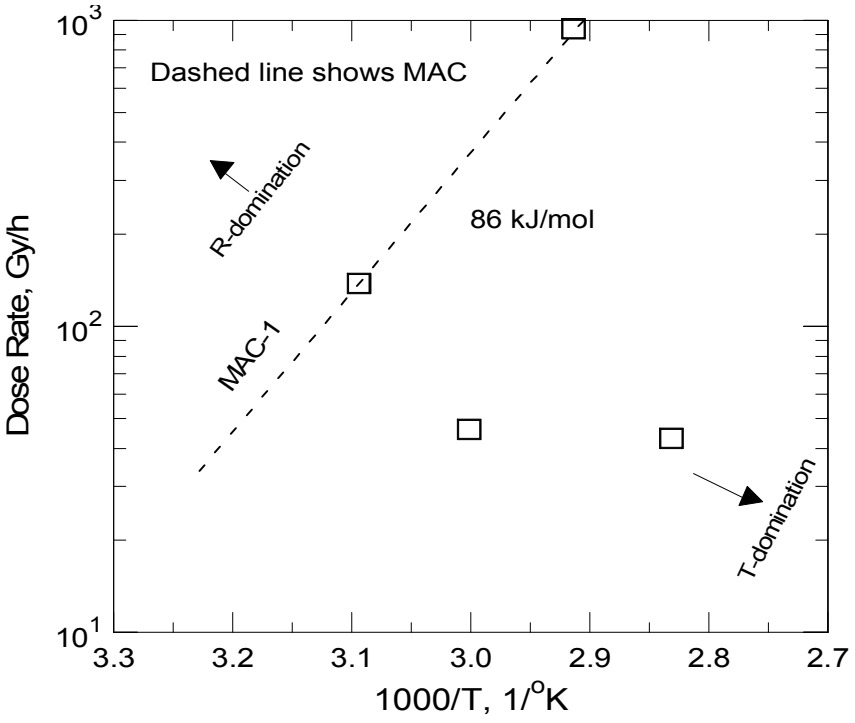

Figure 34. Dose rate and temperature aging conditions for the Rockbestos CR material.

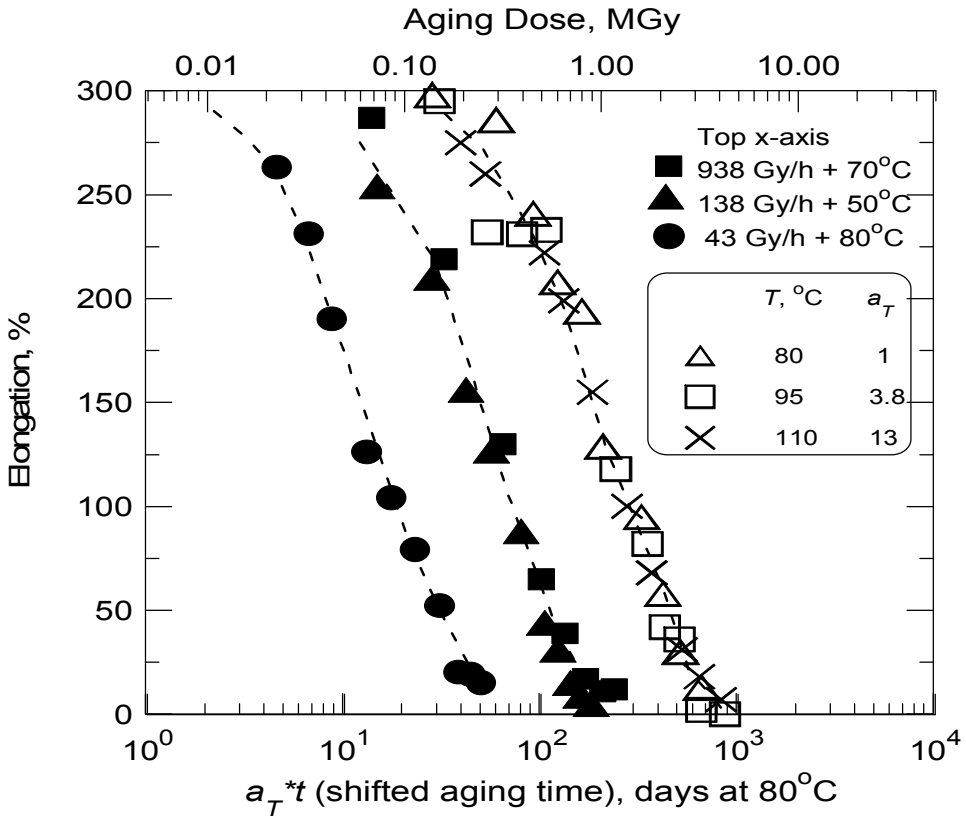

Figure 35. Elongation results for Rockbestos CR. Oven aging results are *t-T* superposed at 80°C (bottom x-axis). Radiation results are plotted (top x-axis) with the same span (10,000) as the lower x-axis.

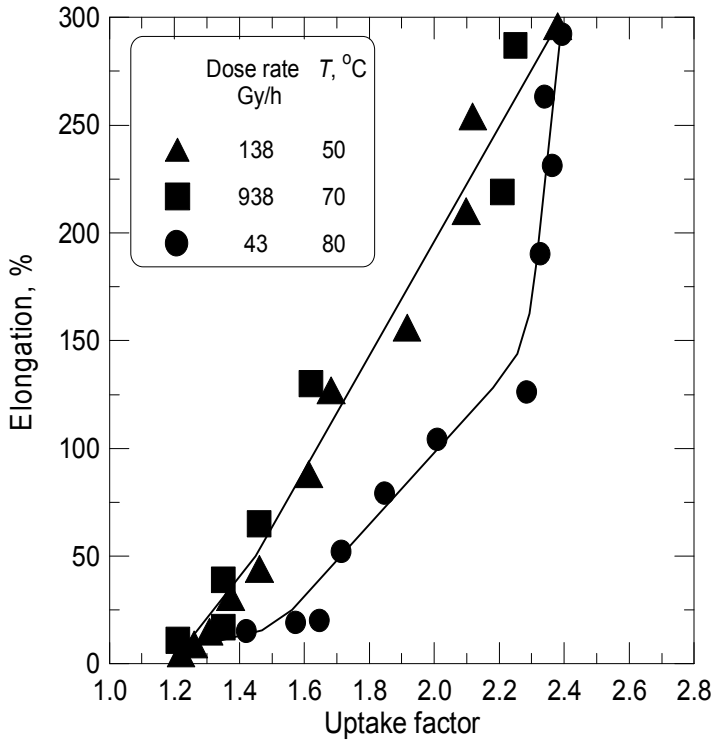

Figure 36. Elongation versus uptake factor for Rockbestos CR at the aging conditions specified.

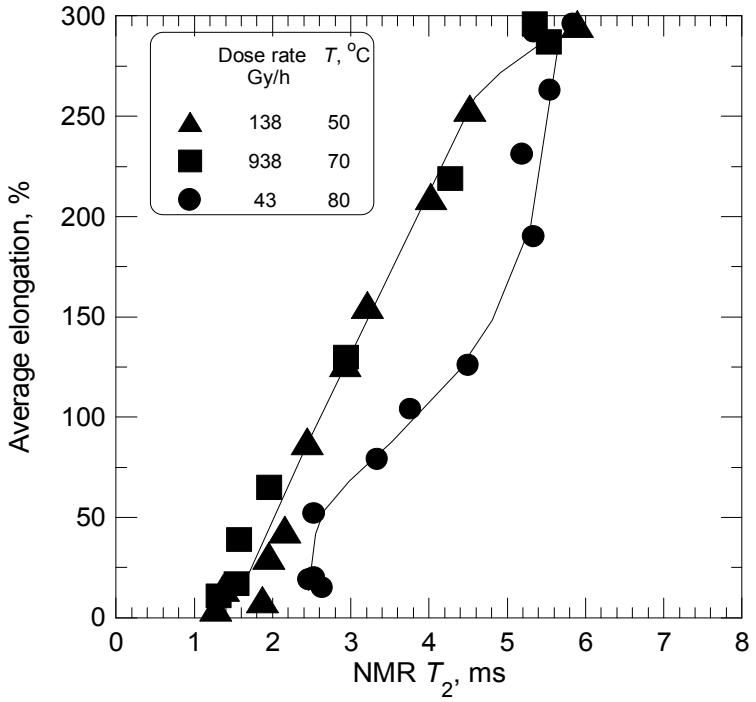

Figure 37. NMR T_2 versus uptake factor for Rockbestos CR at the aging conditions specified.

Summary of MAC approach for accelerated experiments.- Since it should now be clear that the simple assumption underlying the new MAC approach seems to be valid in many instances, a brief review of the approach recommended for simulating given ambient aging conditions will now be given. Suppose one were interested in simulating use conditions of 0.5 Gy/h + 50°C for a material whose oven aging E_a was determined to be 91 kJ/mol. We would first construct a MAC style plot with a "MAC-ambient" line starting at 0.5 Gy/h + 50°C and proceeding to higher dose rate and temperature conditions with a slope equal to 91 kJ/mol. We could choose 20, 50 and 100 times accelerations leading to the experimental conditions shown in Figure 38. By choosing a degradation parameter unaffected by DLO effects, we would next determine whether the experiments at the chosen accelerations (20, 50 and 100x in this example) lead to superposition of the degradation parameter versus dose. If so, we would have confidence that the chemistry was unchanged along the MAC line at least from the 20x acceleration experiment to the 100x acceleration experiment.

Gaining confidence in extrapolations from MAC experiments.- In achieving these goals, we would have resolved two of our earlier three primary issues (unchanged chemistry under the various accelerated conditions and avoiding complications caused by DLO effects). The only remaining issue is the question of how to gain more confidence in the extrapolation of the accelerated results along the MAC line to the ambient condition. This latter goal is achieved in the same manner as done for *T*-only extrapolations, through the use of oxygen consumption measurements both under accelerated conditions and under ambient conditions. The concept is straightforward. Suppose the accelerated results at 20, 50 and 100 times ambient give degradation parameters that superpose when plotted versus dose which says that the chemistry is unchanged at these accelerations. We would then carry out oxygen consumption measurements under ambient conditions and under 20x ambient conditions. If the oxygen consumption rate

was 20 times slower under ambient conditions, this would offer good evidence for a factor of 20 increase in the extrapolated degradation times under ambient conditions. Since this would mean

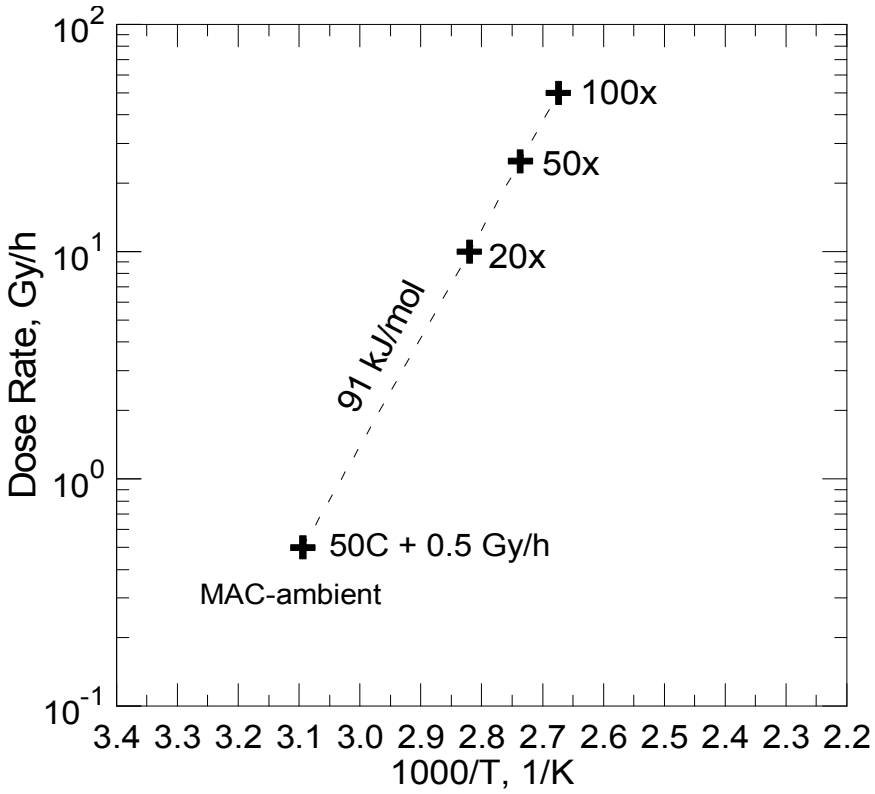

Figure 38. Hypothetical aging conditions to accelerate ambient conditions of 50°C + 0.5 Gy/h by 20, 50 and 100 times using a 91 kJ/mol activation energy for *T*-only experiments.

that the times were increased by a factor of 20 for a MAC reduction in dose rates by as factor of 20, the ambient curve would then be predicted with enhanced confidence to superpose with the accelerated superposed curves when plotted versus dose.

Although this oxygen consumption approach has never been attempted, there exist some results that show the potential promise of this method for gaining confidence in combined environment extrapolations along a MAC line. For the Eaton CSM jacket, oxygen consumption results have been obtained across *R*-*T* space at temperatures ranging from 28°C to 120°C and at dose rates from ~0.5 Gy/h to 300 Gy/h.[29] In Figure 39 we show the results at 28°C and 80°C. The first thing to notice is the excellent sensitivity of the oxygen consumption technique since measurements are available down to very low temperatures and dose rates so that measurements under ambient conditions are readily available. It also should be noted that the data at 80°C levels out at low dose rates corresponding to thermal domination so the leveling out gives the consumption rate at 80°C for *T*-only conditions. The reason we chose the 80°C consumption results is that one of the four *R*+*T* experiments run on Eaton CSM (the point on the MAC-2 line of Figure 28) was an experiment at 56 Gy/h + 80°C. Using this data point and the 91 kJ/mol E_a for the MAC line, we can extrapolate down to 28°C (a factor of 211x decrease from the 91 kJ/mol) to get the MAC corresponding dose rate of 0.265 Gy/h as indicated in Figure 40. We can now use the data from Figure 39 with a slight extrapolation of the 28°C results (Figure 41) to

obtain consumption estimates under the two conditions of interest. The values are 4.2e-11 and 1.95e-13 mol/g/s, respectively which give an experimental ratio of 215. Since this is virtually identical to the factor of 211 predicted, it would give us great confidence in an extrapolation from our 80°C + 56 Gy/h data results to an ambient like condition of 28°C + 0.256 Gy/h.

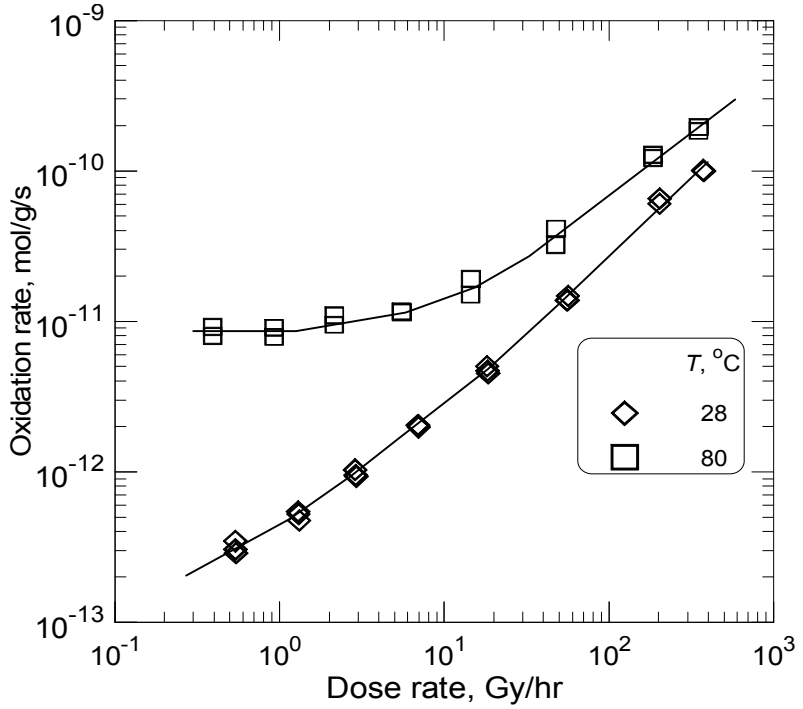

Figure 39. Oxygen consumption results for Eaton CSM versus dose rate and temperature.

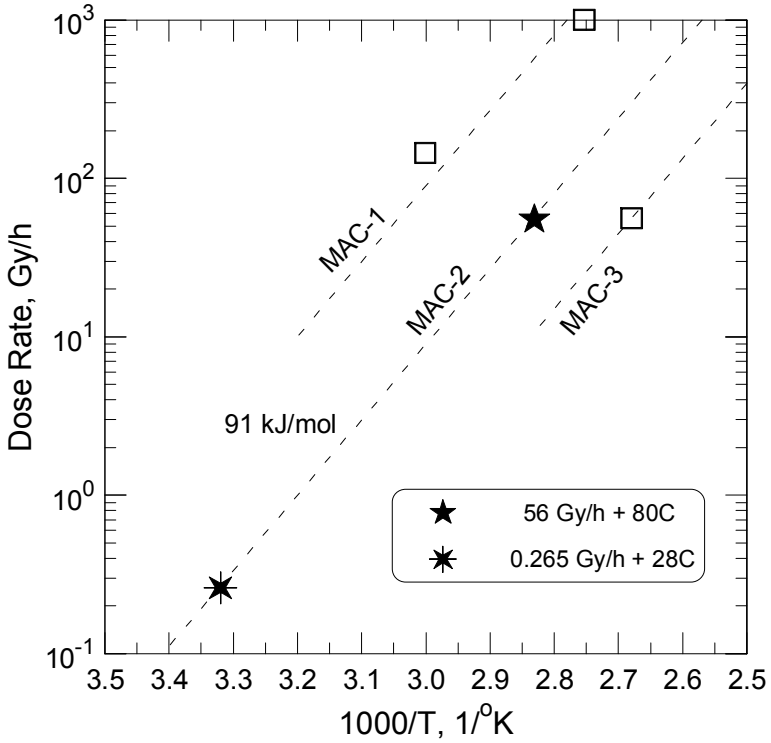

Figure 40. Eaton CSM experimental conditions plus an extrapolation along MAC-2 to 28°C.

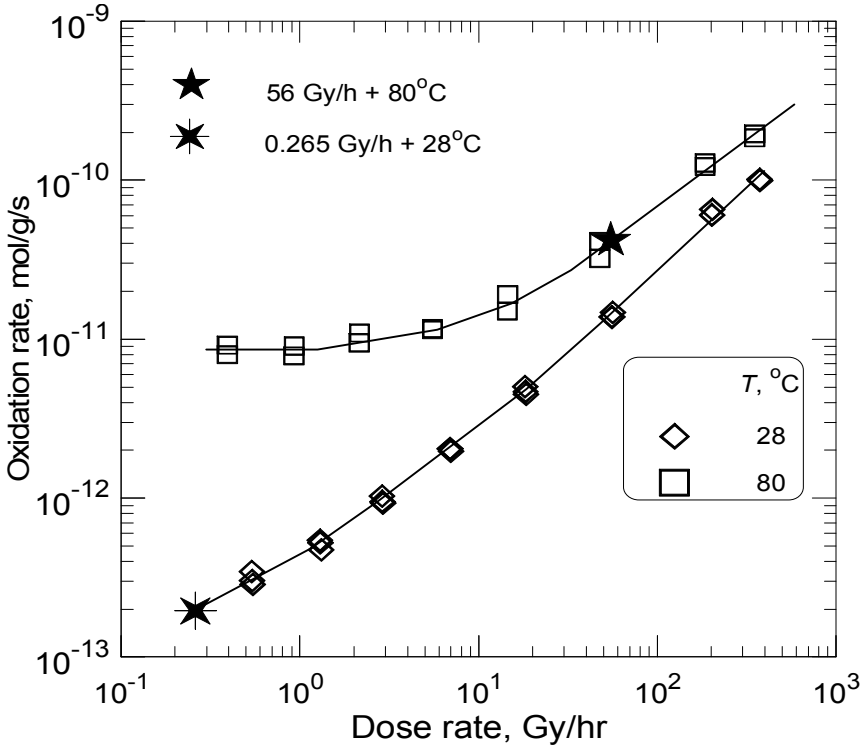

Figure 41. Figure 39 with estimates of consumption at the two marked points.

Wear-out approach for combined environments.- In several past publications, we have introduced and tested what we refer to as the Wear-out approach for thermally-aged materials.[27,30,31] When the chemical degradation reactions remain unchanged (constant degradation shape when time-temperature superposed) over a temperature range, the Wear-out approach assumes that switching aging temperatures in the middle of a sample's degradation will lead to the degradation continuing to follow the *t-T* superposed curve but at the time scale appropriate to the new temperature. As an example, Figure 42 shows *t-T* superposed density results for the aging of an EPM material at four temperatures ranging from 99°C to 139°C.[27] The two x-axes at the bottom of the figure give the times appropriate to the highest and lowest aging temperatures. If a sample has been aging at 99°C for 52 weeks (equivalent to 1 week at 139°C) and we move it to a 139°C oven, we would expect it to continue following the superposed curve using the time scale appropriate to 139°C aging. Thus 1 week of sequential aging at 139°C would be expected to be equivalent to 2 weeks at this temperature for a previously unaged. Similarly 2 weeks sequential would equal 3 weeks non-sequential, etc. If failure was defined when the density rapidly increases, ~ 5 weeks at 139°C would lead to failure for 52 weeks pre-aging at 99°C. Similarly, for 102 weeks pre-aging at 99°C, failure would occur after 4 weeks at 139°C. Thus if the same chemistry held from 99°C to 139°C, a plot of times to failure at 139°C(the Wear-out temperature) vs the pre-aging times at 99°C would be expected to show linear behavior as shown in Figure 43. The potential power of the Wear-out approach concerns situations where accelerated aging extrapolations make predictions for materials expected to survive for long periods of time (decades). In such instances, samples aged under ambient conditions may be available for testing after say 5 years, 10 years, 15 years, etc. The Wear-out approach can be used on these samples to see 1) if their degradation properties track as expected

as discussed in Figure 42 and 2) whether their selected "failure times" lead to linear predictable behavior versus ambient aging time as seen in Figure 43.

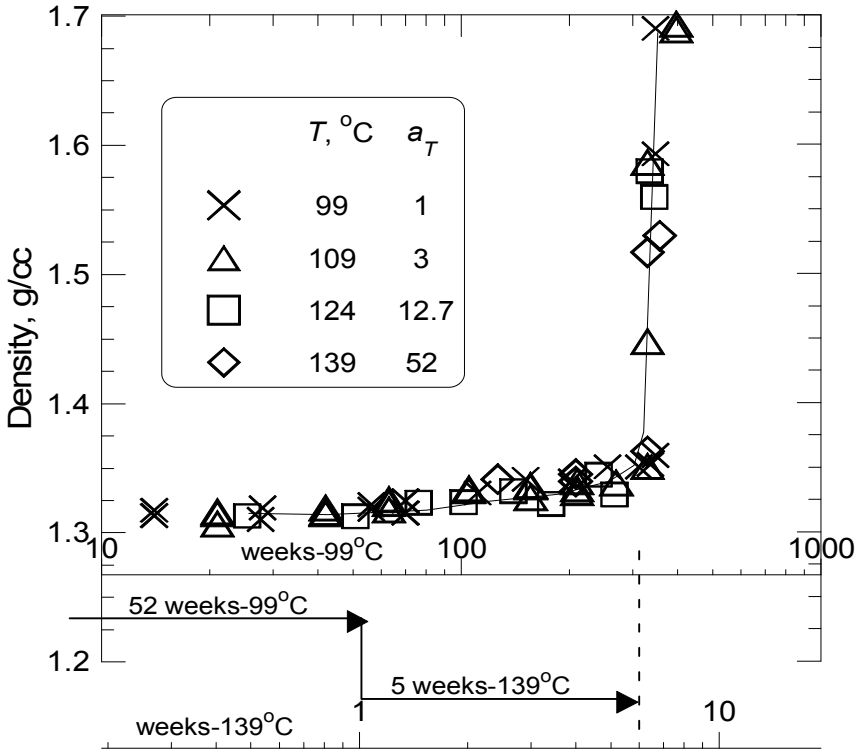

Figure 42. Time-temperature superposition of the density results for an EPM using the empirically derived shift factors shown on the figure. The time-scales appropriate to the highest and lowest aging temperatures are shown below the superposed results.

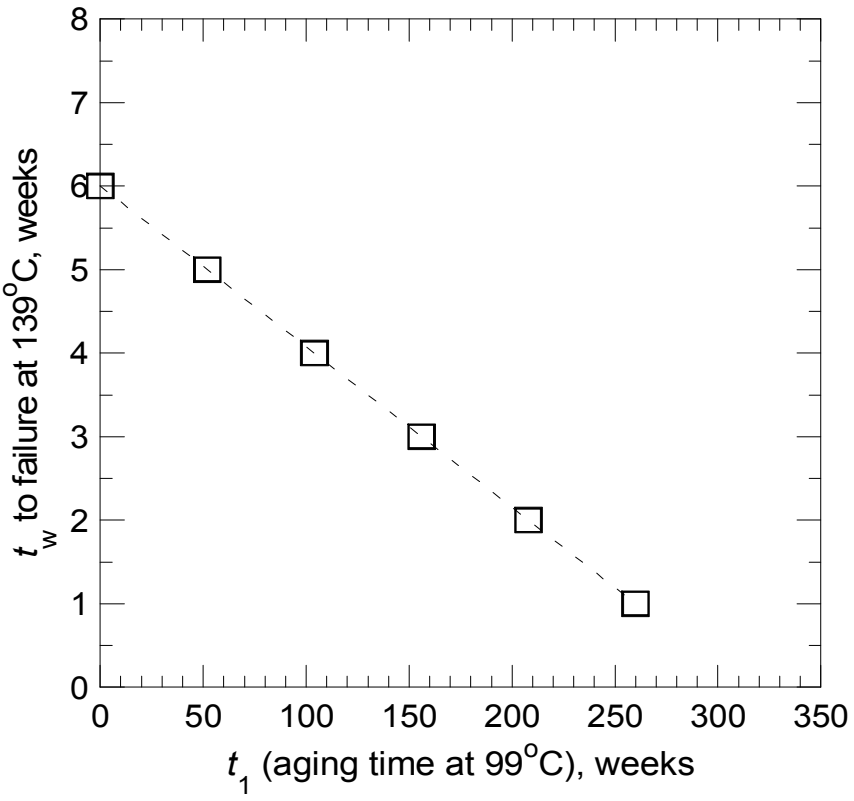

Figure 43. Expected plot for the Wear-out time to failure at 139°C after pre-aging for various times at 99°C if the chemistry does not change over this temperature range.

With the above in mind, it is easy to see how the Wear-out approach can be expanded to handle combined environment situations. The key again is the MAC idea. Assume two or more accelerated conditions on the MAC line that passes through the ambient condition of interest show superposition versus dose. Also assume that oxygen consumption measurements under ambient and accelerated conditions are consistent with MAC predictions for acceleration. In this instance we would have excellent evidence for unchanging chemistry for accelerated $R+T$ conditions and ambient conditions. Thus we would expect the degradation variable to have the same shape versus dose at both accelerated and ambient conditions. With this in mind, Figure 44 shows a hypothetical combined environment elongation versus dose (bottom x-axis) plot analogous to the temperature-only plot in Figure 42. If the time scale for the hypothetical 50x ambient accelerated degradation curve is given by the top most x-axis, a lack of chemistry change at ambient would mean that the ambient time axis would be 50 times longer than the accelerated time axis as shown in the figure by the second upper x-axis. Thus if we received a sample that had seen 10 years at ambient and followed that up with a 50x MAC acceleration for 0 yr, 0.3 yr, 0.7 yr and 1.8 yr, we would expect the results shown on the figure by solid squares. Similarly when a 20 year ambient sample became available, sequential 50x MAC acceleration for 0, 0.3, 0.8 1.1 and 2.1 years would be expected to give the results shown by the Xs on the figure. Clearly such results would add confidence to the extrapolated prediction and give warnings of chemistry changes if the Wear-out results deviated from the predictions. Also, similar to the thermal only case in Figure 43, if we chose a failure criterion (e.g., 50% elongation) and plotted the Wear-out times to this criterion versus the ambient aging times, we would expect linear behavior.

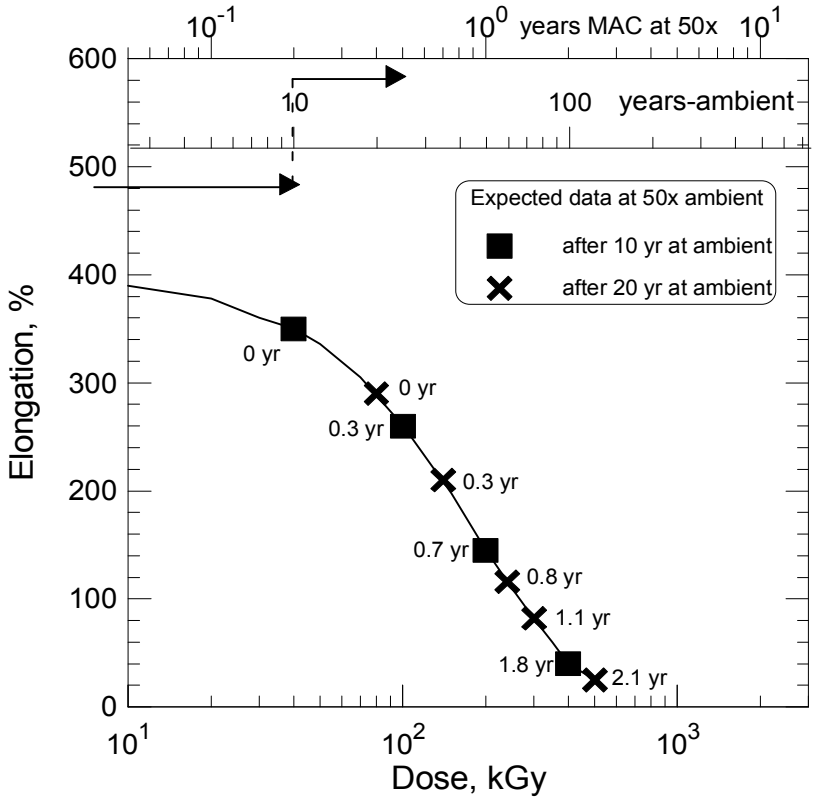

Figure 44. Expected universal degradation plot versus dose along a MAC line if accelerated results show superposition with dose and oxygen consumption results from ambient to accelerated agree with the MAC prediction.

Materials not amenable to MAC approach.- One group of materials that will not be able to be modeled with the MAC approach are a group of materials that show so-called inverse temperature behavior.[32,33] This behavior manifests itself when lowering the combined environment aging temperature at reasonably constant dose rates leads to a faster degradation rate. This usually occurs for temperatures below ~60°C and almost always involves materials with substantial crystallinity. As an example, Figure 45 shows elongation versus dose results for an Eaton EPM aged at similar dose rates at temperatures ranging from 120°C down to 22°C. At the highest temperature (120°C) the degradation occurs quickly. As the temperature is lowered to 100°C and 80°C, degradation doses shift as normally expected to longer and longer doses. However, when the temperature drops to 40°C, the expected trend reverses with degradation occurring more quickly than at 80°C. This inverse-temperature effect continues as the temperature drops further to 22°C. Neither the MAC approach nor any other simple model can handle such strange behavior, presumably caused by transitioning across the crystalline melting point region.

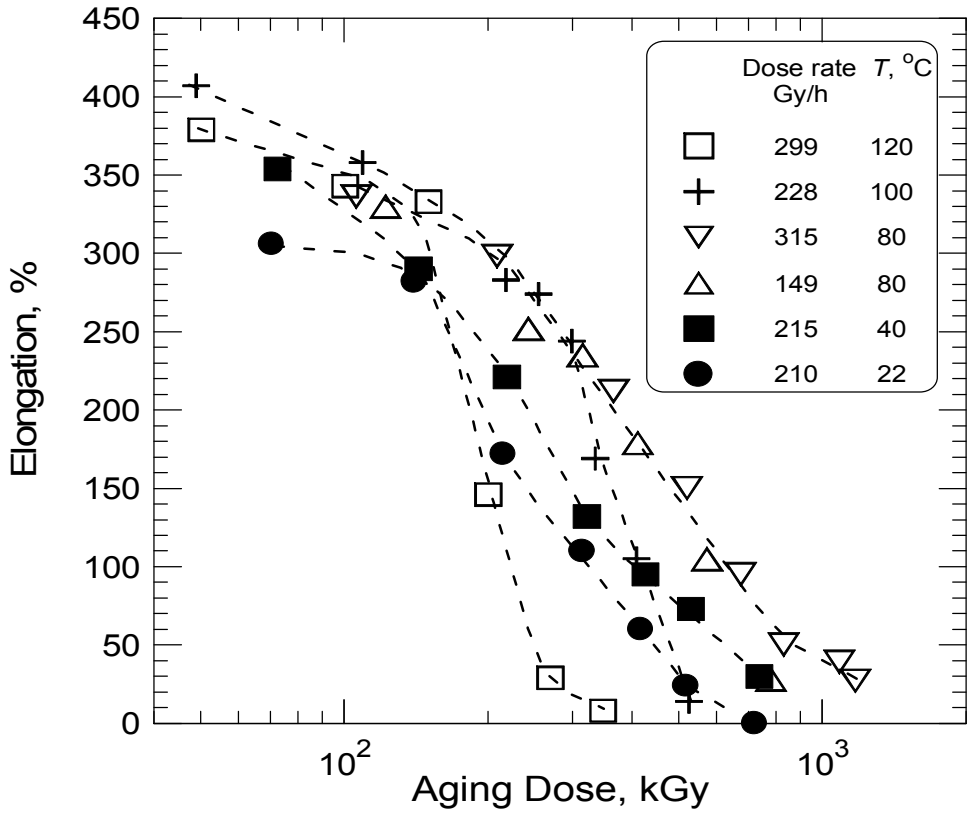

Figure 45. Elongation versus dose for Eaton EPM under the conditions shown.

CONCLUSIONS

Modeling and extrapolating accelerated combined radiation plus temperature (*R*+*T*) environments is a long-standing challenge. We use data from historical combined *R*+*T* studies to show that one of the fundamental difficulties is the observation that the degradation chemistry changes as one moves throughout *R*-*T* space. This observation makes sense when one considers the differences in initiation species expected from thermal versus radiation environments. We therefore conclude that the empirical so-called time-dependent approach, which requires unchanged chemistry across *R*-*T* space, is not a viable approach. We introduced a second approach many years ago involving the assumption that simultaneously accelerating by a factor x both the thermal pathway (using measured Arrhenius shift factors from thermal-only studies) and the radiation pathway (by raising the dose rate *R* by a factor x) will lead to an overall degradation rate increase by the factor x. Although this approach seemed promising, we applied it in a simplistic fashion by using it to analyze a single point on the degradation curve such as the dose required to reach a certain degradation level. Given the observation of chemistry dependent on the location in *R*-*T* space, we have updated our model by introducing Matched Accelerated Conditions (MAC) lines consistent with this assumption on a plot of log *R* versus inverse absolute temperature. If our simple assumption holds, experimental data taken on *R*-*T* points along a MAC line should represent unchanging chemistry except for the acceleration factor x appropriate to each set of points. This implies that all the results along a MAC line should superpose when plotted versus dose, an observation that would also be consistent with the lack of radiation dose rate effects (DRE). We show that this anticipated result is observed by examining dose dependent degradation results along or near several MAC lines for EPM, CR and CSM

elastomers. The MAC approach easily handles the changes in chemistry occurring across *R-T* space and offers a better, more reliable method to assess the potential importance of DRE. We show how the MAC approach can be used to choose accelerated aging conditions that would be expected to represent the same chemistry as the ambient aging conditions of interest along a MAC line that we call the MAC-ambient line. Since oxygen consumption measurements are sensitive enough to allow measurements under most ambient conditions, we next indicate how such measurements under ambient and accelerated conditions along the MAC-ambient line can be used to gain confidence in the extrapolation of the accelerated aging results to ambient aging conditions. When samples aged under ambient conditions are periodically available, we show how to sequentially continue the aging of such samples by choosing accelerated conditions along the MAC-ambient line. This so-called Wear-out approach, analogous to the Wear-out approach used for thermal-only situations, can lead to further confirmation of the extrapolated ambient predictions from accelerated aging studies along the MAC-ambient line. Finally we mention several instances where difficulties applying the MAC approach would be anticipated including 1) following degradation properties that are influenced by diffusion-limited oxidation (DLO), 2) attempting to analyze results for materials with important crystallinity and 3) analyzing results for materials with inverse-temperature effects (often crystalline materials).

ACKNOWLEDGMENTS

Sandia is a multi-program laboratory operated by Sandia Corporation, a Lockheed Martin Company, for the United States Department of Energy's National Nuclear Security Administration under Contract DE-AC04-94AL85000.

REFERENCES

[1] K. T. Gillen, R. Bernstein, and M. Celina, Rubber Reviews. **88**, 1 (2015).
[2] M. Celina, Polym. Degrad. Stab. **98**, 2419 (2013).
[3] K. T. Gillen and R. L. Clough, Polym. Degrad. Stab. **24**, 137 (1989).
[4] K. T. Gillen and R. L. Clough, Radiat. Phys. Chem. **41,** 803 (1993).
[5] S. G. Burnay and J. W. Hitchon, 13th Int. Symp. ASTM STP 956 (Part ii), 609 (1987).
[6] S. Burnay, ACS Symposium Series No, 475, "Radiation Effects on Polymers", R. L. Clough and S. W. Shalaby, Eds., p. 524-533, American Chemical Society (1991).
[7] IEC Technical Report 1244-2. Determination of long-term radiation aging in polymers- Part 2: Procedures for predicting ageing at low dose rates.
[8] IAEA-TECDOC-1188, Vol. II, Annex E (Predictive Modelling of Cable Ageing)
[9] J. Wise, K. T. Gillen, and R. L. Clough, Polym. Degrad. Stab. **49**, 403 (1995).
[10] R. A. Assink, M. Celina, J. M. Skutnik, and D. J. Harris, Polymer, **46**, 11648 (2005).
[11] K. T. Gillen, R. L. Clough, and C. A. Quintana, Polym. Degrad. Stab. **17**, 31 (1987).
[12] K. T. Gillen, E. R. Terrill, and R. W. Winter, Rubber Reviews. **74**, 428 (2001).
[13] K. T. Gillen, R. A. Assink and R. Bernstein, Polym. Degrad. Stab. **84**, 419 (2004).
[14] K. T. Gillen, M. Celina, R. L. Clough, and J. Wise, **Trends in Polymer Science 5**, 250 (1997).
[15] A. V. Cunliffe and A. Davis, Polym. Degrad. Stab. **4**, 17 (1982).
[16] K. T. Gillen and R. L. Clough, Polymer **33**, 4358 (1992).
[17] J. Wise, K. T. Gillen, and R. L. Clough, Polymer **38**, 1929 (1997).
[18] J. D. Ferry, "Viscoelastic Properties of Polymers", John Wiley and Sons, 1970.
[19] K. T. Gillen, unpublished results.

[20] R. L. Clough, K. T. Gillen, and M. Dole, Ch. 3- Radiation Resistance of Polymers and Composites, "Irradiation Effects in Polymers", D. W. Clegg and A. A. Collyer, Eds., Elsevier Science Publishers, Ltd, Essex, England, 1991.
[21] K. T. Gillen, R. Bernstein, R. L. Clough, and M. Celina, Polym. Degrad. Stab. **91**, 2146 (2006).
[22] M. Celina, K. T. Gillen, and E. R. Lindgren, "Nuclear Power Plant Cable Materials: Review of Qualification and Currently Available Aging Data for Margin Assessments in Cable Performance", SANDIA REPORT- SAND2013-2388 (May, 2013).
[23] T. Seguchi and Y. Yamamoto, JAERI 1299, March, 1986.
[24] K. T. Gillen and R. L. Clough, Polymer **33**, 4358 (1992).
[25] R. L. Clough and K. T. Gillen, J. Polym. Sci., P. C. Ed. 23, 359 (1985).
[26] K. T. Gillen and R. L. Clough, Radiat. Phys. Chem., 18, 679 (1981).
[27] K. T, Gillen, R. A. Assink, and R. Bernstein, "Nuclear Energy Plant Optimization (NEPO) Final Report on Aging and Condition Monitoring of Low-Voltage Cable Materials", SANDIA REPORT, SAND2005-7331 (November, 2005).
[28] K. T. Gillen, R. Bernstein, and D. K. Derzon, Polymer Degradation and Stability, 87, 57 (2005).
[29] M. Celina, unpublished.
[30] K. T. Gillen and M. Celina, Polym. Degrad. Stab. **71**, 15 (2001).
[31] K. T. Gillen, M. Celina, R. Bernstein, and M. Shedd, Polym. Degrad. Stab. **91**, 3197 (2006).
[32] M. Celina, K. T. Gillen, J. Wise, and R. L. Clough, Radiat. Phys. Chem. **48**, 613 (1996).
[33] M. Celina, K. T. Gillen, and R. L. Clough, Polym. Degrad. **61**, 231 (1998).

Need page break before listing of all figures

Figure Captions

Figure Error! Main Document Only.**. Arrhenius plot of induction times for an EPDM o-ring material.**
Figure Error! Main Document Only.**.**